

A potential-flow theory for the dynamics of cylinder arrays in cross-flow

By M. P. PAÏDOUSSIS, D. MAVRIPLIS† AND S. J. PRICE

Department of Mechanical Engineering, McGill University,
817 Sherbrooke Street West, Montreal, Québec, Canada

(Received 3 May 1983 and in revised form 21 January 1984)

The full linear unsteady potential-flow solution for fluid flowing across a bank of cylinders has been obtained. The potential function is expanded into a Fourier series and the boundary condition of impermeability is applied at the moving cylinder surfaces. Mutual contradictions among the various potential-flow solutions available in the literature are exposed, and it is shown that the present solution is consistent with certain basic physical checks, which some of the previous solutions could not meet. The effect of fluid viscosity is incorporated solely as a phase lag between the steady-state lift and drag coefficients on each cylinder and its respective motions. By incorporating the fluid-dynamic forces obtained from this modified potential-flow theory in a stability analysis, the threshold for fluid-elastic instability is predicted. Comparison with experimentally observed thresholds is encouraging, given the high level of idealization of the theory and the accuracy of present-day semi-empirical prediction methods.

1. Introduction

Arrays of cylinders, in various geometrical arrangements (figure 1), are commonly found in a variety of industrial equipment; e.g. in heat exchangers and steam generators in the form of tubes containing the primary fluid flow and subjected to an external cross-flow by the secondary fluid. Such systems have, for a long time now, been known to be subject to a number of interesting and, from the practical viewpoint, undesirable flow-induced vibration phenomena; yet the state of understanding of the fluid mechanics and of the fluid-structure interaction mechanisms associated with these phenomena is still quite primitive (Paidoussis 1980, 1981).

It is now generally accepted that there are three types of vibration of cylinder arrays, induced by cross-flow: (i) those due to buffeting; (ii) those due to flow periodicity in the interstitial flow, sometimes reinforced acoustically; (iii) the so-called fluid-elastic instability. This latter, which is the subject of this paper, is a self-excited fluid-elastic phenomenon, involving coupling between the flow field and cylinder motions. At a given threshold flow velocity, energy transfer from the flowing fluid to the cylinders leads to amplified oscillations – i.e. to an instability in the linear sense. The amplitude of these oscillations is generally large, often resulting in intercylinder impact and hence eventually to failure. From the practical point of view, fluid-elastic instability is by far the most serious vibration problem in heat-exchange equipment (Paidoussis 1980). More to the point, there is considerable interest at the fundamental level as to the underlying mechanism associated with this phenomenon. (It is

† Present address: Department of Mechanical and Aerospace Engineering, Princeton University, Princeton, N.J., U.S.A.

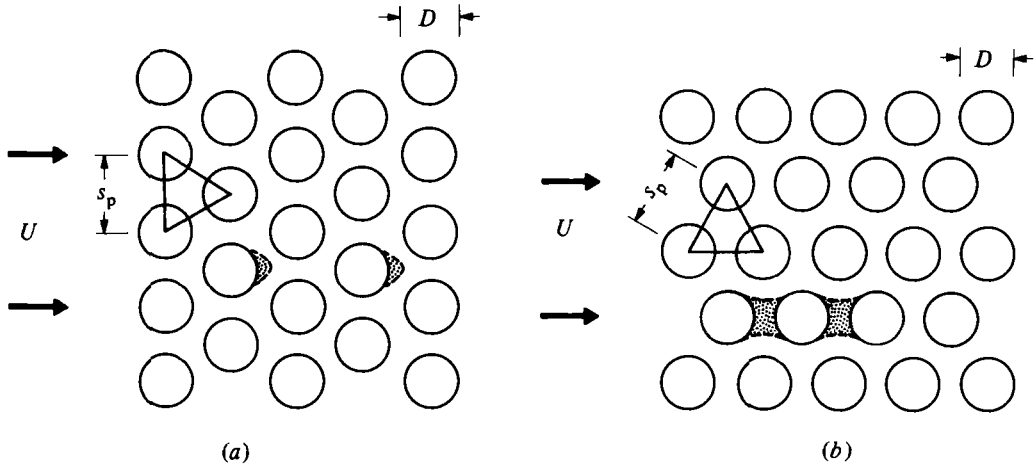


FIGURE 1. Two types of staggered arrays of cylinders in cross-flow: (a) 'normal'; (b) 'parallel', or 'rotated', equilateral triangular array. The dimensionless pitch ratio is defined as s_p/D . Also shown are the separated (rotational) flow regions behind two cylinders in each case.

unfortunate, perhaps, that the severe financial and safety repercussions of failure and shutdown of large power-generating facilities, caused by fluid-elastic instabilities, have created a demand for instant predictive design tools for avoiding them; as a result, in the now voluminous literature on the subject, empirical *ad hoc* studies greatly outnumber the few attempts to gain understanding at the fundamental level.)

Several models have been proposed for the mechanism underlying fluid-elastic instability. Roberts (1962, 1966) demonstrated the existence of a Coanda-like, jet-switching/coalescence mechanism in the separated flow behind an alternately staggered cylinder row, associated with streamwise motions of alternate cylinders, and showed that this is capable of producing large-amplitude self-excited oscillations. Although Roberts' elegant analytical model correlated well with his own experimental data, the existence of bistable jets is considered to be limited to specific array geometries; in any event, the model has not been extended to deal with multi-row arrays.

Connors (1970) generated a semi-empirical, quasi-static model for a single row of cylinders, based on a position-dependent mechanism, and involving the use of measured aerodynamic lift- and drag-coefficient data – both in the equilibrium configuration and in 'deformed' configurations, with some cylinders displaced in the streamwise or cross-stream directions. Connors found that, for certain patterns of intercylinder displacements, energy may be extracted from the fluid over a cycle of cylinder oscillations; when this exceeds the internal dissipative energy in the cylinders, then instability will develop. This model was later elaborated upon and conceptually extended to multi-row arrays by Blevins (1974, 1977). Connors and Blevins obtained a simple relation for the critical flow velocity U_c , for the onset of fluid-elastic instability, namely

$$\frac{U_c}{fD} = K \left\{ \frac{m\delta}{\rho D^2} \right\}^{\frac{1}{2}}, \quad (1)$$

where ρ is the fluid density, D and m are respectively the diameter and mass per unit length of the cylinders, and f and δ are the frequency and logarithmic decrement of vibration of the cylinders. The dimensionless 'reduced velocity' U/fD and 'mass-

damping parameter' $m\delta/\rho D^2$ arise quite commonly and naturally in many aeroelastic studies. Nevertheless, it should be stressed that in this case *all the fluid mechanics* of the problem is absorbed into the empirical factor K . Equation (1) gained widespread acceptance because of its simplicity, as well as success in some cases, and a great deal of effort has subsequently been devoted to empirically developing 'more reliable' and 'more appropriate' (for different array geometries) values of K , separating $m/\rho D^2$ from δ and adjusting the exponents on each in (1), etc. (Pettigrew, Sylvestre & Campagna 1978; Weaver & El Kashlan 1981; Paidoussis 1981).

Tanaka & Takahara (1981) recognized the limitations of Connors' quasi-static hypothesis, and obtained good agreement between their own experiments and theory, by measuring the full unsteady fluid-dynamic forces on cylinders in a water tunnel and using them in a linear analysis – which bespeaks of the high quality of their measurements.

Whereas the above-mentioned work has been more or less successful in determining the critical flow velocities for design purposes, it offers little insight into the actual physical phenomena taking place. It ought to be mentioned that Connors' analysis implicitly supposes that the fluid-dynamic stiffness terms play a predominant role in inducing the instability. This is in contrast to aerodynamic-damping-induced instabilities, e.g. in Den Hartog's (1932) much praised quasi-static model for galloping of iced transmission lines. With this observation in mind, Price & Paidoussis (1982, 1983) proposed a similar quasi-static flutter mechanism for a double-row array, into which measured aerodynamic stiffness and damping coefficients are incorporated. The critical flow velocity is found to be dependent on, among other things, array geometry, fluid/cylinder density ratio and intercylinder modal pattern. The relationship for U_c/fD is more complex than that of (1), and this theory is in agreement with a number of experimental observations.

In a recent, remarkable study Chen (1983*a, b*) suggests that two different mechanisms are responsible for fluid-elastic instability: in liquid flow, given the low flow velocities necessary for precipitating the instability, the ratio of cylinder vibrational velocity to the mainstream flow velocity is high, and hence the prevailing mechanism is one of flutter by negative hydrodynamic damping; in gaseous flow, on the other hand, the Connors–Blevins mechanism predominates, which is an aerodynamic-stiffness-controlled mechanism involving at least two degrees of freedom. His analysis requires knowledge of the unsteady fluid force coefficients; using Tanaka & Takahara's (1981) data, Chen's results compare favourably with experimental data in both liquid- and gaseous-flow cases. Recently, Lever & Weaver (1982) proposed yet another model, in which fluid-elastic instability is presumed to be a unique mechanism arising from interstitial flow redistribution, associated with and lagging behind cylinder motions. The results obtained agree remarkably with Chen's, despite the fundamental differences in the two models, as well as with experimental trends for some array geometries; nevertheless, some important disagreements also arise (Paidoussis 1983; Heinecke & Mohr 1982).

Flow-visualization experiments by one of the authors (Mavriplis 1982), as well as earlier work by Wallis (1939), have shown that for some array geometries the wakes behind the cylinders are quite narrow, especially when intercylinder spacing is small – as sketched in figure 1 (*a*). The presence of adjacent cylinders seems to deflect fluid into the wake of upstream cylinders, minimizing the regions of rotational flow and resulting in surprisingly potential-like flow distributions. Hence, it is rather tempting and not so outrageous to try analysing the system as if the flow were entirely

inviscid.† Dalton & Helfinstine (1971) arrived at an inviscid solution by considering each cylinder as a doublet in uniform flow, plus the appropriate image doublets due to mutual interaction of the cylinders, thus obtaining an infinite-series velocity-potential function. However, their analysis becomes overlaborious for systems of more than a few cylinders, and singularities arise for closely spaced cylinders; moreover, in their work no attention has been given to the question of instabilities. Balsa (1977) solved the potential-flow problem for a general array of cylinders in cross-flow by utilizing matched-asymptotic-expansion techniques. A model for predicting static instability (divergence) is also presented, although the dynamic (flutter) instability is not given any attention. Comparison between theoretical and experimental results is very limited.

Chen (1978) tackled the same problem, solving the Laplace equation in terms of infinite Fourier series, subject to the impermeability boundary conditions at the surface of each cylinder. Examples of predicted inertial, fluid-dynamic damping and stiffness terms are presented, and they are found to compare poorly with experiments. A full stability analysis is also given, but no results are published. However, it is felt that in this solution several important terms have been neglected, as will be discussed later, raising questions as to the validity of the results.

The three aforementioned potential-flow theories have been found (see §5) to be in disagreement with one another, in terms of some important features of the results obtained, ‡ indicating that they cannot all be wholly correct. An aim of the present paper is to resolve these discrepancies, by carefully rederiving the potential-flow solution for the problem at hand and testing it along the way in every conceivable manner. It is then possible to pursue the more general aim of this paper, which is to explore further the capabilities and limitations of potential-flow theory for dealing with the dynamical behaviour of cylinder arrays in cross-flow.

2. Formulation of the flow field

The analysis to be presented is, in principle at least, valid for all array geometries; however, because of the narrowness of the wakes in the so-called ‘normal triangular’ configuration of figure 1(a), it is expected to be most successful for that geometry and especially when the cylinders are closely spaced, i.e. when s_p/D is small. Figure 2 defines the various geometrical parameters, as well as the coordinate systems used: one inertial set (r_i, θ_i) centred on each cylinder at its position of equilibrium, and another (r'_i, θ'_i) moving with each cylinder in addition to the central inertial Cartesian and polar systems (x, y) and (r_0, θ_0) .

It is assumed that the flow field is represented by the potential function Φ , with one component due to the mainstream cross-flow and the other due to the presence/motion of each cylinder j , i.e.

$$\Phi(r, \theta, t) = Ur_0 \cos(\theta_0 - \psi_0) + \sum_{j=1}^K \phi_j(r, \theta, t), \quad (2)$$

† In the case of axial flow about cylinders and cylinder arrays, where rotational flow regions are rather small, potential-flow theory has been eminently successful in predicting the dynamical behaviour and stability characteristics of the system (Paidoussis 1966*a, b*; 1979).

‡ For example, the velocity-dependent self-damping force, produced on itself by motion of a cylinder in the array, is found to be perpendicular to cylinder motion by Dalton & Helfinstine (1971), whilst Chen’s (1978) theory predicts components both normal and parallel to cylinder motion; Balsa’s (1977) solution, on the other hand, indicates that this force is zero.

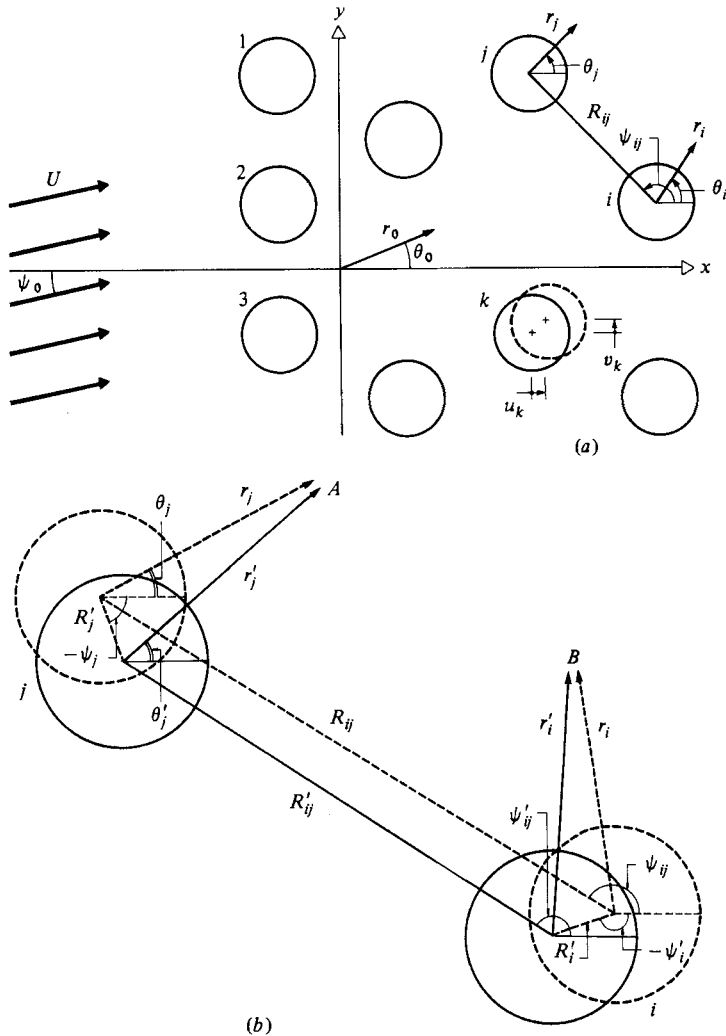


FIGURE 2. (a) The system under consideration, with the associated coordinate systems (x, y) , (r_0, θ_0) , (r_j, θ_j) , the geometric parameters R_{ij} , ψ_{ij} , and cylinder displacements u_k, v_k , defined therein; (b) the coordinate systems (r'_i, θ'_i) , (r'_j, θ'_j) , moving with each cylinder, *vis à vis* the fixed ones, (r_i, θ_i) , (r_j, θ_j) , and associated definitions.

where K is the number of cylinders in the system. As Φ must satisfy the Laplace equation, it is convenient to express the ϕ_j in terms of Fourier series; thus for the j th cylinder

$$\phi_j = \sum_{n=1}^{\infty} \frac{R^{n+1}}{r_j'^n} \{a_{jn} \cos n\theta'_j + b_{jn} \sin n\theta'_j\} \tag{3}$$

in terms of the moving coordinate system centred on that cylinder, where it is noted that $\phi_j \rightarrow 0$ as $r'_j \rightarrow \infty$. The total velocity potential Φ must satisfy the condition of impermeability at the surface of the cylinders, i.e.

$$\left. \frac{\partial \Phi}{\partial r'_i} \right|_{r'_i=R} = \frac{\partial u_i}{\partial t} \cos \theta'_i + \frac{\partial v_i}{\partial t} \sin \theta'_i \quad (i = 1, 2, \dots, K), \tag{4}$$

where u_i and v_i are the Cartesian displacements of cylinder i in the x - and y -directions respectively. The constants a_{jn} , b_{jn} are determined through application of this

boundary condition, and to facilitate this endeavour the following expansions are found useful:

$$\left. \begin{aligned} a_{jn} &= \sum_{l=1}^K \left\{ \alpha_{jnl} \left(\frac{\partial u_l}{\partial t} - U \cos \psi_0 \right) + \gamma_{jnl} \left(\frac{\partial v_l}{\partial t} - U \sin \psi_0 \right) \right\}, \\ b_{jn} &= \sum_{l=1}^K \left\{ \delta_{jnl} \left(\frac{\partial u_l}{\partial t} - U \cos \psi_0 \right) + \beta_{jnl} \left(\frac{\partial v_l}{\partial t} - U \sin \psi_0 \right) \right\}, \end{aligned} \right\} \quad (5)$$

so that the task now becomes to determine $\alpha_{jnl}, \dots, \delta_{jnl}$.

Before applying the boundary conditions, however, all the ϕ_j must be expressed in the moving coordinate frame centred on each of the cylinders in turn. Thus, for the j th potential to be expressed in the coordinate frame associated with the moving cylinder i , one may use the vectorial relationship

$$r'_j \exp(i\theta'_j) = r'_i \exp(i\theta'_i) - R'_{ij} \exp(i\psi'_{ij}),$$

as is evident from figure 2 when points A and B coincide, where $i = \sqrt{-1}$; this, raised to the power $-n$ and expanded into a convergent Taylor series about $r'_i/R'_{ij} = 0$ (Paidoussis & Suss 1977; Mavriplis 1982), after considerable manipulation leads to

$$\frac{\cos n\theta'_j}{r_j'^n} = \sum_{m=0}^{\infty} \frac{(-1)^n (n+m-1)! r_i'^m}{m! (n-1)! R'_{ij}{}^{m+n}} \cos [m\theta'_i - (n+m)\psi'_{ij}], \quad (6)$$

and to a similar expression for $\sin n\theta'_j/r_j'^n$. With the aid of these expressions, ϕ_j in (3) is transformed into the (r'_i, θ'_i) coordinate system, and one finally obtains

$$\begin{aligned} \Phi &= U r_0 \cos(\theta_0 - \psi_0) + \sum_{n=1}^{\infty} \frac{R^{n+1}}{r_i'^n} \{a_{in} \cos n\theta'_i + b_{in} \sin n\theta'_i\} \\ &+ \sum_{j=1}^K * \sum_{n=1}^{\infty} \sum_{m=0}^{\infty} \frac{(-1)^n (n+m-1)! R^{n+1} r_i'^m}{m! (n-1)! R'_{ij}{}^{m+n}} \\ &\times \{a_{jn} \cos [m\theta'_i - (m+n)\psi'_{ij}] - b_{jn} \sin [m\theta'_i - (m+n)\psi'_{ij}]\}, \end{aligned} \quad (7)$$

where the starred summation excludes $j = i$.

Substituting (5) into (7), and then applying the boundary conditions (4), and after lengthy manipulation and extensive use of the orthogonality of $\cos m\theta'_i$ and $\sin m\theta'_i$, the following implicit expressions for the coefficients $\alpha_{jnl}, \dots, \delta_{jnl}$ are finally found:

$$\left. \begin{aligned} (-n) \alpha_{inl} + \sum_{j=1}^K * \sum_{m=1}^{\infty} G'_{mnij} \{ \alpha_{jml} \cos((m+n)\psi'_{ij}) + \delta_{jml} \sin((m+n)\psi'_{ij}) \} &= \delta_{n1} \delta_{il}, \\ (-n) \delta_{inl} + \sum_{j=1}^K * \sum_{m=1}^{\infty} G'_{mnij} \{ \alpha_{jml} \sin((m+n)\psi'_{ij}) - \delta_{jml} \cos((m+n)\psi'_{ij}) \} &= 0, \\ (-n) \gamma_{inl} + \sum_{j=1}^K * \sum_{m=1}^{\infty} G'_{mnij} \{ \gamma_{jml} \cos((m+n)\psi'_{ij}) + \beta_{jml} \sin((m+n)\psi'_{ij}) \} &= 0, \\ (-n) \beta_{inl} + \sum_{j=1}^K * \sum_{m=1}^{\infty} G'_{mnij} \{ \gamma_{jml} \sin((m+n)\psi'_{ij}) - \beta_{jml} \cos((m+n)\psi'_{ij}) \} &= \delta_{n1} \delta_{il}, \end{aligned} \right\} \quad (8)$$

for $i = 1, 2, \dots, K$ and $l = 1, 2, \dots, K$, and $n = 1, 2, \dots, \infty$, where

$$G'_{mnij} = \frac{(-1)^m (n+m-1)! \left(\frac{R}{R'_{ij}}\right)^{n+m}}{(n-1)! (m-1)!}, \quad (9)$$

and δ_{n1}, δ_{il} is Kronecker's delta. This represents $2K$ sets of $2K \times \infty$ coupled equations, with as many unknowns. Truncating the series at appropriate values of m and n , the coefficients $\alpha_{jnl}, \dots, \delta_{jnl}$ may clearly be determined numerically.

Once Φ is determined, the surface pressure on each cylinder at its position of equilibrium may be obtained from the unsteady Bernoulli equation

$$P|_{r'_i=r_i=R} = -\rho \left[\frac{\partial \Phi}{\partial t} + \frac{1}{2} \nabla \Phi \cdot \nabla \Phi \right]_{r'_i=r_i=R}, \tag{10}$$

and hence the fluid-dynamic forces acting on cylinder i are

$$H_i = - \int_0^{2\pi} P|_{r_i=R} R \cos \theta_i d\theta_i, \quad V_i = - \int_0^{2\pi} P|_{r_i=R} R \sin \theta_i d\theta_i \tag{11}$$

in the x - and y -directions respectively. Evaluation of (10) would, at first sight, appear to be quite straightforward; however, if sufficient care is not exercised, it may lead to erroneous results, as discussed in §3.

3. Evaluation of the unsteady pressure field on the surface of the cylinders

In a previous study (Chen 1978) the $\partial \Phi / \partial t$ term in (10) was found to yield only inertial terms – i.e. terms proportional to $\partial^2 u_i / \partial t^2$, $\partial^2 v_i / \partial t^2$. However, velocity-dependent terms (fluid-dynamic damping terms) also arise from $\partial \Phi / \partial t$, but this was not realized in that previous analysis through failure to use the moving coordinate frames (r'_j, θ'_j) , rather than those (r_j, θ_j) fixed at equilibrium.

The manner in which these velocity-dependent terms arise may be illustrated by considering the simple case of a single cylinder in inviscid cross-flow. This system may be represented by either (i) a stationary doublet in uniform flow, with a complex potential function $F(z) = Uz + UR^2/z$, or (ii) a moving doublet in otherwise stationary fluid, where $F(z) = UR^2/[z - \zeta(t)]$ and $\zeta(t) = -Ut$. The surface-pressure distribution in both cases is found by applying

$$P|_{z=R} = -\rho \left\{ \frac{\partial \Phi}{\partial t} + \frac{1}{2} \nabla \Phi \cdot \nabla \Phi \right\} + \text{const}, \tag{12}$$

with $\Phi = \text{Re}\{F(z)\}$.

Now, in the first case, the potential function is time-independent, and hence $\partial \Phi / \partial t = 0$. Evaluation of $\nabla \Phi \cdot \nabla \Phi$ then leads to the well-known result

$$P|_{z=R} = \frac{1}{2} \rho U^2 (1 - 4 \sin^2 \theta) + \text{const}, \tag{13}$$

where it may be shown that the constant represents P_∞ , the static pressure far away.

In case (ii), if it is assumed that the doublet passes through the origin at $t = 0$, one obtains $\nabla \Phi \cdot \nabla \Phi|_{z=R} = U^2$. Thus, if $(\partial \Phi / \partial t)_{t=0}$ is neglected, then, in spite of the fact that there is no acceleration of the cylinder, the correct pressure distribution cannot be obtained. In fact, it may be shown that $(\partial \Phi / \partial t)_{t=0} = -U^2 \cos 2\theta$, thus leading once more to (13), provided that the terms in (12) are correctly interpreted.

Thus it has been shown that $\partial \Phi / \partial t$ is important in determining not only fluid-dynamic inertial (acceleration) terms, but also velocity-dependent terms. As the cylinders in the problem at hand are moving, moving reference frames must be utilized; the various terms in (10) may be taken at equilibrium in all cases, except for the $\partial \Phi / \partial t$ term, which is evaluated at equilibrium *after* the differentiation (with respect to time) is performed. More explicitly, in differentiating equations of the form of (7), terms such as $\cos n\theta'_i / r'_i$ and the α_{jnl} , β_{jnl} implicit in the a_{jn} , b_{jn} must be considered to be time-dependent.

The $\nabla \Phi \cdot \nabla \Phi$ term in (10) yields additional fluid-dynamic damping forces,† as well

† Of course (10) gives the pressure, which only when integrated through (11) leads to forces. It is, however, convenient to thus identify the terms that eventually lead to these forces.

as the steady lift and drag forces due solely to the cross-flow. In addition there will be terms dependent on the displacement of each and every cylinder, i.e. the fluid-dynamic stiffness terms.

Evaluation of the $\partial\Phi/\partial t$ term

Expanding the sine and cosine terms of (7), $\partial\Phi/\partial t$, evaluated at the cylinder equilibrium positions (i.e. $R'_{ij} = R_{ij}$, $\psi'_{ij} = \psi_{ij}$, $r'_i = r_i$, $\theta'_i = \theta_i$), may be written as

$$\begin{aligned} \frac{\partial\Phi}{\partial t} = & \sum_{n=1}^{\infty} \frac{R^{n+1}}{r_i^n} (\dot{a}_{in} \cos n\theta_i + \dot{b}_{in} \sin n\theta_i) \\ & + \sum_{n=1}^{\infty} R^{n+1} \left\{ a_{in} \left(\frac{\cos n\theta'_i}{r_i'^n} \right)' + b_{in} \left(\frac{\sin n\theta'_i}{r_i'^n} \right)' \right\} \\ & + \sum_{j=1}^K \sum_{n=1}^{\infty} \sum_{m=0}^{\infty} \frac{(-1)^n (m+n-1)! R^{n+1}}{m!(n-1)! R_{ij}^{m+n}} r_i^m \\ & \quad \times [\{\dot{a}_{jn} \cos(m+n)\psi_{ij} + \dot{b}_{jn} \sin(m+n)\psi_{ij}\} \cos m\theta_i \\ & \quad + \{\dot{a}_{jn} \sin(m+n)\psi_{ij} - \dot{b}_{jn} \cos(m+n)\psi_{ij}\} \sin m\theta_i] \\ & + \sum_{j=1}^K \sum_{n=1}^{\infty} \sum_{m=0}^{\infty} \frac{(-1)^n (m+n-1)! R^{n+1}}{m!(n-1)! R_{ij}^{m+n}} \\ & \quad \times [\{a_{jn} \cos(m+n)\psi_{ij} + b_{jn} \sin(m+n)\psi_{ij}\} (r_i'^m \cos m\theta'_i)' \\ & \quad + \{a_{jn} \sin(m+n)\psi_{ij} - b_{jn} \cos(m+n)\psi_{ij}\} (r_i'^m \sin m\theta'_i)'] \\ & + \sum_{j=1}^K \sum_{n=1}^{\infty} \sum_{m=0}^{\infty} \frac{(-1)^{n+1} (m+n)! R^{n+1}}{m!(n-1)! R_{ij}^{m+n+1}} \dot{R}_{ij} r_i^m \\ & \quad \times [\{a_{jn} \cos(m+n)\psi_{ij} + b_{jn} \sin(m+n)\psi_{ij}\} \cos m\theta_i \\ & \quad + \{a_{jn} \sin(m+n)\psi_{ij} - b_{jn} \cos(m+n)\psi_{ij}\} \sin m\theta_i] \\ & + \sum_{j=1}^K \sum_{n=1}^{\infty} \sum_{m=0}^{\infty} \frac{(-1)^n (m+n)! R^{n+1}}{m!(n-1)! R_{ij}^{m+n}} r_i^m \dot{\psi}_{ij} \\ & \quad \times [\{-a_{jn} \sin(m+n)\psi_{ij} + b_{jn} \cos(m+n)\psi_{ij}\} \cos m\theta_i \\ & \quad + \{a_{jn} \cos(m+n)\psi_{ij} + b_{jn} \sin(m+n)\psi_{ij}\} \sin m\theta_i], \end{aligned} \tag{14}$$

where $(\quad)' = \partial(\quad)/\partial t$.

Each of the dotted terms has to be evaluated separately. Thus, using (5), one may write

$$\dot{a}_{jn} = \sum_{l=1}^K [\alpha_{jnl} \ddot{u}_l + \gamma_{jnl} \ddot{v}_l] + \sum_{l=1}^K [\dot{\alpha}_{jnl} (\dot{u}_l - U \cos \psi_0) + \dot{\gamma}_{jnl} (\dot{v}_l - U \sin \psi_0)], \tag{15}$$

where

$$\dot{\alpha}_{jnl} = \sum_{l'=1}^K \left[\frac{\partial \alpha_{jnl}}{\partial u_{l'}} \dot{u}_{l'} + \frac{\partial \alpha_{jnl}}{\partial v_{l'}} \dot{v}_{l'} \right] \tag{16}$$

and a similar expression holds for $\dot{\gamma}_{jnl}$. Clearly, terms proportional to $U\dot{u}_l$ and $U\dot{v}_l$ arise, i.e. damping terms which were neglected in the aforementioned previous analysis. The lengthy manipulations necessary for obtaining \dot{a}_{jn} and \dot{b}_{jn} , which also

necessitate the evaluation of \dot{R}_{ij} and $\dot{\psi}_{ij}$, are outlined in Appendix A. The $(\partial\alpha_{jnl}/\partial u_v)$, etc., terms are given by the implicit equations

$$\begin{aligned}
 -n \left(\frac{\partial\alpha_{jnl}}{\partial u_v} \right) + \sum_{j=1}^K \sum_{m=1}^{\infty} G_{mnij} \left\{ \left(\frac{\partial\alpha_{jnl}}{\partial u_v} \right) \cos [(m+n)\psi_{ij}] + \left(\frac{\partial\delta_{jnl}}{\partial u_v} \right) \sin [(m+n)\psi_{ij}] \right\} &= P_{inlv}, \\
 -n \left(\frac{\partial\delta_{jnl}}{\partial u_v} \right) + \sum_{j=1}^K \sum_{m=1}^{\infty} G_{mnij} \left\{ \left(\frac{\partial\alpha_{jnl}}{\partial u_v} \right) \sin [(m+n)\psi_{ij}] + \left(\frac{\partial\delta_{jnl}}{\partial u_v} \right) \cos [(m+n)\psi_{ij}] \right\} &= Q_{inlv},
 \end{aligned}$$

where P_{inlv} , Q_{inlv} are given in Appendix A, with similar expressions for the rest of the u_v and v_v derivatives of α_{jnl} , β_{jnl} , γ_{jnl} and δ_{jnl} . Furthermore, \dot{R}_{ij} and $\dot{\psi}_{ij}$ are given by (A 2) and (A 3) respectively.

Next, in order to evaluate the dotted terms in the second and fourth summations of (14), the terms of the type $\cos n\theta'_i/r'_i$ and $r'_i{}^m \cos m\theta'_i$ must first be expressed in terms of the stationary frame (r_i, θ_i) . This is done in a similar manner to that used to obtain (6), but the expansion is made about $R'_i/r_i = 0$, yielding

$$\begin{aligned}
 \frac{\cos n\theta'_i}{r'_i} &= \sum_{m=n}^{\infty} \frac{(m-1)! R'_i{}^{m+n}}{(n-1)! (m-n)! r_i^m} \cos [m\theta_i - (m-n)\psi'_i], \\
 r'_i{}^m \cos m\theta'_i &= \sum_{n=0}^m \frac{(-1)^{m-n} m! R'_i{}^{m-n} r_i^n}{n! (m-n)!} \cos [n\theta_i + (m-n)\psi'_i],
 \end{aligned}$$

and similar expressions for the sine terms. Differentiating with respect to time and evaluating at $R'_i = 0$, i.e. at equilibrium, gives

$$\left. \begin{aligned}
 \left(\frac{\cos n\theta'_i}{r'_i{}^n} \right)' &= nr_i^{-(n+1)} \dot{R}'_i \cos [(n+1)\theta_i - \psi'_i], \\
 (r'_i{}^m \cos m\theta'_i)' &= -mr_i^{m-1} \dot{R}'_i \cos [(m-1)\theta_i + \psi'_i],
 \end{aligned} \right\} \tag{17}$$

where it is further noted (figure 2) that

$$\dot{R}'_i \cos \psi'_i = \frac{\partial u_i}{\partial t}, \quad \dot{R}'_i \sin \psi'_i = \frac{\partial v_i}{\partial t}. \tag{18}$$

Hence, with all the dotted quantities evaluated, $\partial\Phi/\partial t$ may be found. The contribution to the forces on the cylinders due to this term, denoted by $H_i^{(1)}$ and $V_i^{(1)}$, are somewhat simplified – after lengthy manipulation – due to orthogonality of the trigonometric functions, and are given by

$$\left. \begin{aligned}
 H_i^{(1)} &= \rho\pi R^2 \sum_{l=1}^K [A_{il}\ddot{u}_l + B_{il}\ddot{v}_l] + \rho UR \sum_{l=1}^K [\{C_{il}^{(1)} + C_{il}^{(2)}\} \dot{u}_l + \{D_{il}^{(1)} + D_{il}^{(2)}\} \dot{v}_l], \\
 V_i^{(1)} &= \rho\pi R^2 \sum_{l=1}^K [\bar{A}_{il}\ddot{u}_l + \bar{B}_{il}\ddot{v}_l] + \rho UR \sum_{l=1}^K [\{\bar{C}_{il}^{(1)} + \bar{C}_{il}^{(2)}\} \dot{u}_l + \{\bar{D}_{il}^{(1)} + \bar{D}_{il}^{(2)}\} \dot{v}_l],
 \end{aligned} \right\} \tag{19}$$

where the superscript (1) denotes terms arising from time derivatives of α , β , γ , δ , and (2) denotes those arising from coordinate-system movement. The constants A_{il} , B_{il} , etc. are given in Appendix B. It is noted that in Chen's (1978) previous analysis all the terms involving \dot{u}_l and \dot{v}_l are absent.

Evaluation of $\nabla\Phi \cdot \nabla\Phi$ term

The flavour, intricacy and requisite care in the derivation of the terms in (10) may be appreciated from the foregoing evaluation of $\partial\Phi/\partial t$. In the interests of brevity,

therefore, the details of the derivation of the $\nabla\Phi \cdot \nabla\Phi$ term will not be presented here. The interested reader is referred for details to Mavriplis (1982) and Chen (1978).

It may be shown that the contributions of $\nabla\Phi \cdot \nabla\Phi$ to the drag and lift forces on cylinder i , denoted by $H_i^{(2)}$ and $V_i^{(2)}$, are

$$\left. \begin{aligned} H_i^{(2)} &= \rho U^2 R C_{D0i} + \rho UR \sum_{l=1}^K \{C_{il}^{(3)} \dot{u}_l + D_{il}^{(3)} \dot{v}_l\}, \\ V_i^{(2)} &= \rho U^2 R C_{L0i} + \rho UR \sum_{l=1}^K \{\bar{C}_{il}^{(3)} \dot{u}_l + \bar{D}_{il}^{(3)} \dot{v}_l\}, \end{aligned} \right\} \quad (20)$$

where C_{D0i} and C_{L0i} are the steady drag and lift coefficients and $C_{il}^{(3)}, \dots, \bar{D}_{il}^{(3)}$ are coefficients of additional velocity-dependent terms, expressions for which are given in Appendix B.

Evaluation of the stiffness forces

The stiffness forces represent the changes in the steady lift and drag on the cylinders as they are displaced. Assuming that they may be linearized, the contribution to the lift and drag forces may be expressed by

$$\left. \begin{aligned} H_i^{(3)} &= \rho U^2 R \sum_{p=1}^K \left\{ \frac{\partial C_{D0i}}{\partial u_p} u_p + \frac{\partial C_{D0i}}{\partial v_p} v_p \right\}, \\ V_i^{(3)} &= \rho U^2 R \sum_{p=1}^K \left\{ \frac{\partial C_{L0i}}{\partial u_p} u_p + \frac{\partial C_{L0i}}{\partial v_p} v_p \right\}, \end{aligned} \right\} \quad (21)$$

where the partial-derivative terms are given in Appendix B; for detailed derivations the reader is referred to Mavriplis (1982).

In all the foregoing it has been assumed that pressure fluctuations on the surface of the cylinders are generated instantaneously; i.e. it has been presumed that there is no phase difference between cylinder displacements and the pressure field, otherwise known as the quasi-static assumption. Yet, it has been shown that phase lags do arise in the problem at hand – at least in the model proposed by Roberts (1962, 1966). In that work, Roberts evaluated the finite time necessary for the intercylinder fluid jets to adjust to repositioning of the cylinders, as well as the resulting change in the cylinder wake (or ‘bubble’) pressure. Here the phase lag may be thought to be related to viscous effects more generally, i.e. to the lag that the cylinder wake experiences in adjusting to cylinder motion. In terms of the mean-flow velocity U and cylinder diameter D , this time lag should be proportional to D/U , and hence the phase-lag angle χ should be proportional to fD/U , where f is the frequency of oscillation (cf. Lever & Weaver 1982; White 1979).

Thus, although viscous forces *per se* will not be calculated and used in this analysis – having been assumed to be of secondary importance at the outset of this paper – one important *effect* of these forces will be incorporated in the analysis, namely the phase-lag effect discussed above, which modifies the quasi-static forces. The analogy of the aerofoil could be invoked here: the viscous forces in that case are small and may be neglected; yet they have a very important effect in determining the structure of the flow and modifying the inviscid forces – hence determining the Kutta condition.†

† Phase lag is well known to have an important effect on stability in aero-elasticity. Thus, in addition to the aforementioned work by Roberts (1966) and recent work by Lever & Weaver (1982) on the problem at hand, note the importance of phase lag – albeit due to mechanisms different from the one proposed here – in flutter of aerofoils (Bisplinghoff, Ashley & Halfman 1955; Dowell *et al.* 1980) and of overhead transmission lines (Simpson & Flower 1977).

If the cylinders oscillate harmonically only in the cross-stream direction, such that $v_p = \bar{v}_p \sin(\omega t + \phi_p)$, then the forces $H_i^{(3)}$, $V_i^{(3)}$ will also vary harmonically, but lagging by a phase angle χ , so that

$$H_i^{(3)} = \rho U^2 R \sum_{p=1}^K \left(\frac{\partial C_{D0i}}{\partial v_p} \right) \bar{v}_p \sin(\omega t + \phi_p + \chi),$$

which may be rewritten as

$$H_i^{(3)} = \rho U^2 R \sum_{p=1}^K \left(\frac{\partial C_{D0i}}{\partial v_p} \right) \left\{ \cos \chi v_p + \frac{\sin \chi}{\omega} \dot{v}_p \right\}, \quad (22)$$

and similarly for $V_i^{(3)}$. The generalization to more general motions is self-evident, yielding

$$\left. \begin{aligned} H_i^{(3)} &= \rho U^2 R \sum_{p=1}^K \left\{ [E_{ip} \cos \chi u_p + F_{ip} \cos \chi v_p] + \left[E_{ip} \frac{\sin \chi}{\omega} \dot{u}_p + F_{ip} \frac{\sin \chi}{\omega} \dot{v}_p \right] \right\}, \\ V_i^{(3)} &= \rho U^2 R \sum_{p=1}^K \left\{ [\bar{E}_{ip} \cos \chi u_p + \bar{F}_{ip} \cos \chi v_p] + \left[\bar{E}_{ip} \frac{\sin \chi}{\omega} \dot{u}_p + \bar{F}_{ip} \frac{\sin \chi}{\omega} \dot{v}_p \right] \right\}, \end{aligned} \right\} \quad (23)$$

where

$$E_{ip} = \frac{\partial C_{D0i}}{\partial u_p}, \quad F_{ip} = \frac{\partial C_{D0i}}{\partial v_p}, \quad \bar{E}_{ip} = \frac{\partial C_{L0i}}{\partial u_p}, \quad \bar{F}_{ip} = \frac{\partial C_{L0i}}{\partial v_p},$$

and where the cylinders have been assumed to oscillate harmonically; ω is the vibration frequency of the cylinders at the threshold of instability.† Hence, yet another set of velocity-dependent forces, of the form of the second terms of (23), emerge, related to this phase lag.

4. The equations of motion and their solution

If each of the cylinders is considered to be a simple beam, then the equations of motion may be written in the form

$$\left. \begin{aligned} EI \frac{\partial^4 u_i}{\partial z^4} + c \frac{\partial u_i}{\partial t} + m \frac{\partial^2 u_i}{\partial t^2} &= \sum_{l=1}^K \left\{ \rho \pi R^2 \left[A_{il} \frac{\partial^2 u_l}{\partial t^2} + B_{il} \frac{\partial^2 v_l}{\partial t^2} \right] \right. \\ &\quad \left. + \rho UR \left[C_{il} \frac{\partial u_l}{\partial t} + D_{il} \frac{\partial v_l}{\partial t} \right] + \rho U^2 R [E_{il} u_l + F_{il} v_l] \right\} + \rho U^2 R C_{D0i}, \\ EI \frac{\partial^4 v_i}{\partial z^4} + c \frac{\partial v_i}{\partial t} + m \frac{\partial^2 v_i}{\partial t^2} &= \sum_{l=1}^K \left\{ \rho \pi R^2 \left[\bar{A}_{il} \frac{\partial^2 u_l}{\partial t^2} + \bar{B}_{il} \frac{\partial^2 v_l}{\partial t^2} \right] \right. \\ &\quad \left. + \rho UR \left[\bar{C}_{il} \frac{\partial u_l}{\partial t} + \bar{D}_{il} \frac{\partial v_l}{\partial t} \right] + \rho U^2 R [\bar{E}_{il} u_l + \bar{F}_{il} v_l] \right\} + \rho U^2 R C_{L0i}, \end{aligned} \right\} \quad (24)$$

for $i = 1, 2, \dots, K$, where EI , c and m are respectively the flexural rigidity, internal (viscous) damping and mass per unit length of each cylinder; the right-hand sides of the equations are respectively $H_i = H_i^{(1)} + H_i^{(2)} + H_i^{(3)}$, $V_i = V_i^{(1)} + V_i^{(2)} + V_i^{(3)}$, where the component terms $H_i^{(1)}$, $H_i^{(2)}$, etc. have been derived in §3 – in general also containing phase-related terms of the form introduced in (23).

† It should be noted, however, that in the calculations ω will simply be taken as the natural frequency of the cylinders, to avoid the complication of iterative eigenvalue solution procedures. The justification for this is that, for oscillatory instabilities at least, the vibration frequency at the instability threshold is very close to the natural frequency (see e.g. Paidoussis 1980, 1981).

The solution of the linearized form of (24) is achieved by the modal-analysis method (Bishop & Johnson 1960), where

$$u_i = \sum_{p=1}^{\infty} q_{ip}(t) \psi_p(z), \quad v_i = \sum_{p=1}^{\infty} r_{ip}(t) \psi_p(z), \quad (25)$$

where the $\psi_p(z)$ are the orthonormal set of beam eigenfunctions of the cylinders *in vacuo*. Substituting into (24), invoking the orthogonality of the $\psi_p(z)$, and truncating the series at an appropriate value of p , one eventually obtains a set of equations which may be written in matrix form as follows

$$\mathbf{M}\ddot{\mathbf{a}} + \mathbf{C}\dot{\mathbf{a}} + \mathbf{K}\mathbf{a} = \mathbf{0}, \quad (26)$$

where $\mathbf{a} = \{\mathbf{q}, \mathbf{r}\}^T$. Transforming this into a standard eigenvalue problem, the $2K$ eigenvalues of the system may be obtained, which permits one to assess stability of the system with varying U .

The detailed forms of \mathbf{M} , \mathbf{C} and \mathbf{K} will not be given here. Suffice it to say that, when (26) is written in dimensionless form, the following dimensionless quantities will be involved: the mass parameter $m/\rho D^2$; the logarithmic decrement δ of the cylinders *in vacuo*; the reduced velocity U/fD , where $f = \omega/2\pi$ is the first-mode *in vacuo* frequency, ω being the corresponding radian frequency; the frequency ratio $\xi_p = \omega_p/\omega$, where ω_p is the radian frequency of the p th mode.

5. Testing the potential-flow solution

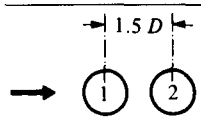
Although an attempt has been made in the foregoing to incorporate viscous effects by introducing a phase lag, the major part of this work involves the derivation of the purely inviscid potential-flow solution for the system under consideration. As this solution is known to be unique and as apparent contradictions have been found to exist between various previous solutions for this problem, it is imperative to undertake extensive testing of this aspect of the theory, prior to embarking on a full-scale stability analysis.

Apart from verifying that some obvious symmetry conditions imposed by various cylinder geometries are indeed reproduced in the calculated force coefficients, various other simple tests were also conducted. Thus, the flow at zero incidence ($\psi_0 = 0$ – see figure 2) across a particular array was reproduced by rotating the array through an angle ψ_0 and imposing an angle of incidence ψ_0 to the flow.

It was then attempted to compare the various fluid force coefficients in (19)–(24) with those obtained by other analyses. The virtual- (added-) mass coefficients A_{ii} , \bar{A}_{ii} , B_{ii} , \bar{B}_{ii} were compared with those obtained by Chen (1975, 1978), Suss (1977), Paidoussis & Suss (1977) and Dalton & Helfinstine (1971). The coefficients were found to agree to within three significant figures for the first two, and to within two significant figures for the third one, as illustrated in table 1. The steady lift and drag coefficients were also compared to some available theoretical results by Chen and Dalton & Helfinstine, in table 1, displaying similarly good agreement.

The portions of the damping coefficients due to the $\nabla\Phi \cdot \nabla\Phi$ term in Bernoulli's equation, i.e. $C_{ii}^{(3)}$, $\bar{C}_{ii}^{(3)}$, $D_{ii}^{(3)}$, $\bar{D}_{ii}^{(3)}$, which have also been obtained by Chen (1978), were compared in the case of a five-cylinder system. Some selected results are shown in the upper part of table 2, where agreement is found to obtain to three significant figures.

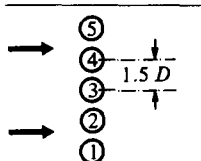
The total fluid-damping coefficients C_{ii} , D_{ii} , \bar{C}_{ii} , \bar{D}_{ii} cannot be verified, as no other potential-flow results are available in the literature. However, some simplified cases



		Present analysis	Chen (1978)	Suss (1977)	Dalton & Helfinstine (1971)
Inertia terms ($\bar{A}_{ii} = \bar{B}_{ii} = 0$)	A_{11}	-1.0320	-1.0325	-1.0328	-1.0313†
	A_{12}	0.2269	0.2265	0.2266	0.2245†
	\bar{B}_{11}	-1.0320	-1.0325	-1.0328	-1.0313†
	\bar{B}_{12}	-0.2269	-0.2265	-0.2266	-0.2245†
Steady lift and drag coefficients	C_{D0i}	-0.3464	-0.3493	—	-0.3474‡
	C_{L0i}	0	0	—	—

† Obtained by Mavriplis (1982), using Dalton & Helfinstine's analysis.
‡ Obtained graphically.

TABLE 1. Comparison of the inertia terms and steady lift and drag forces predicted by the present analysis with those obtained by various other authors in the published literature



		Present analysis	Chen (1978)
Damping terms	$C_{23}^{(3)}$	0	0
	$D_{23}^{(3)}$	-0.7478	-0.747
	$\bar{C}_{23}^{(3)}$	-0.9510	-0.950
	$\bar{D}_{23}^{(3)}$	0	0
Stiffness terms	E_{23}	1.090	1.089
	F_{23}	0	0
	\bar{E}_{23}	0	0
	\bar{F}_{23}	-1.657	-1.650

TABLE 2. Certain damping terms due to the steady part of Bernoulli's equation ($\nabla\Phi \cdot \nabla\Phi$) and some stiffness terms, obtained analytically by the present analysis, compared with those of Chen (1978), obtained by displacing one cylinder at a time, for the five-cylinder row shown

may be verified by a specially constructed quasistatic analysis. Thus, if all cylinders move with the same velocities \dot{u} and \dot{v} in the x - and y -directions, the array configuration remains unchanged, as the whole array is displaced as a unit. Without giving details of the analysis here, which follows the pattern of Den Hartog's (1932) quasi-static flutter analysis (see Price & Paidoussis 1983; Mavriplis 1982), suffice it to say that the unsteady drag and lift forces on the cylinders are found to be given by

$$H_i = \rho UR \left\{ -2C_{D0i} \dot{u}_i + \left(C_{L0i} + \frac{\partial C_{D0i}}{\partial \alpha} \right) \dot{v}_i \right\},$$

$$V_i = \rho UR \left\{ -2C_{L0i} \dot{u}_i + \left(-C_{D0i} + \frac{\partial C_{L0i}}{\partial \alpha} \right) \dot{v}_i \right\},$$

with $\dot{u}_i = \dot{u}$, $\dot{v}_i = \dot{v}$ for all i , and $\alpha \approx \dot{v}/U$. The $\partial C_{L0i}/\partial \alpha$ and $\partial C_{D0i}/\partial \alpha$ terms arise because, under the effect of the imposed motion, the array is not totally symmetric *vis à vis* the mean flow; i.e. the angle α effectively corresponds to $-\psi_0$. Agreement between the results obtained by the potential-flow analysis and this quasi-static approach was found to be excellent, the individual terms agreeing to within four

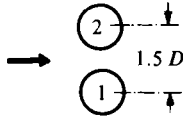
significant figures. This represents an important feature of this analysis, as not all previous analyses pass this simple test.

It must nevertheless be noted that, in the above case where the array is moved as a unit, there is no intercylinder motion. Hence, only the $C_{ii}^{(2)}$, $D_{ii}^{(2)}$ types of terms in (19) are verified, and it would be desirable to test independently the terms of the types $C_{ii}^{(1)}$, $D_{ii}^{(1)}$, which are associated with the α_{jni} , β_{jni} , γ_{jni} , δ_{jni} terms (see (16)). To this end, the changes to the α_{jni} , ..., δ_{jni} , i.e. the $\partial\alpha_{jni}/\partial u_j$, etc., have been calculated by displacing each cylinder by a small amount Δu at the input stage of the computer program and recalculating all the α_{jni} , ..., δ_{jni} coefficients at each step, thus obtaining $\partial\alpha_{jni}/\partial u_j \approx \Delta\alpha_{jni}/\Delta u_j$. This somewhat inelegant and approximate evaluation of the $\partial\alpha_{jni}/\partial u_j$ and other similar terms permitted the eventual evaluation of the $C_{ii}^{(1)}$ type of terms. Comparisons of these terms with those obtained analytically by the potential-flow analysis are illustrated in table 3. Acceptable agreement is obtained; most of the discrepancies are thought to arise from the finite step size of Δu (or Δv).

In spite of all the above testing, the theory still did not agree with that of Balsa (1977). Regardless of cylinder array configuration, the present analysis yields zero diagonals in the C_{ii} and \bar{D}_{ii} submatrices, while the diagonal of the D_{ii} submatrix is non-zero and equal to the negative of the \bar{C}_{ii} diagonal. Physically, this implies that the motion of any one cylinder in an array produces a force on itself which is perpendicular to its motion, and precludes the possibility of any self-damping forces on the cylinder in the direction of its motion. A cylinder can, however, produce damping forces in any direction on the other cylinders regardless of its motion. This result disagrees with that obtained in the work of Balsa (1977). By constructing inner- and outer-region canonical potentials for a cylinder array and matching them asymptotically, Balsa arrived at the result that the motion of any one cylinder in the array produces no net damping force on itself in either direction, i.e. the diagonals of all submatrices C_{ii} , \bar{C}_{ii} , D_{ii} , \bar{D}_{ii} are zero. After the extensive testing performed on the present analysis, it is felt that the fault must lie in Balsa's work rather than in this analysis.† Balsa's expansions are expressed in powers of ϵ , where $\epsilon = D/s_p$ is the inverse of the pitch ratio. In performing the asymptotic matching, three inner terms and four outer terms are used. However, for pitch ratios of order 1.5, the fourth term in the expansion, ϵ^4 , is approximately 0.2. Hence, at first view, it seems Balsa may have neglected significant higher-order terms. (In fact, the diagonals of D_{ii} , \bar{C}_{ii} , which vanish in Balsa's analysis, are always substantially smaller than unity in the present analysis.) However, the above is only a possible explanation of the inconsistency between the two analyses, and the matter has not been pursued further.

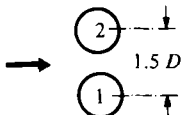
Nevertheless, to ensure that the present analysis is not in error, the method of Dalton & Helfinstine (1971) was employed to calculate the damping terms in the simple case of a row of two cylinders normal to the flow. The method consists of constructing the complex potential function by considering one doublet for each cylinder moving in still fluid, plus its image in the neighbouring cylinder, which is required to maintain a circular streamline at the neighbouring cylinder boundary, plus the images of the images and so on. For the two cylinders at a pitch ratio of 1.5, a total of six doublets was employed (i.e. up to 'third order'), since the third-order images were about 1% of the strength of the original doublet. The complex potential function was obtained through a specially written computer program, and its time derivative calculated by first evaluating the complex potential on the moving cylinder boundaries at two different times and then dividing the difference by the

† Although it is realized that neither truly represents the physics of the situation, as an oscillating cylinder will be subjected to a damping force due to its own motion.



	Cylinder-displacement method $\Delta u = 0.004D$	Analytical calculation
$[D_{ii}^{(1)}]$	$\begin{bmatrix} 0.3292 & -0.3258 \\ 0.3292 & -0.3258 \end{bmatrix}$	$\begin{bmatrix} 0.3791 & -0.3791 \\ 0.3791 & -0.3791 \end{bmatrix}$
$[\bar{D}_{ii}^{(1)}]$	$\begin{bmatrix} 0.2376 & -0.2376 \\ 0.2376 & -0.2376 \end{bmatrix}$	$\begin{bmatrix} 0.1992 & -0.1992 \\ 0.1992 & -0.1992 \end{bmatrix}$

TABLE 3. Comparison of the potential flow damping terms due to the time derivatives of the α_{jn} , ..., δ_{jn} coefficients obtained analytically with those obtained by displacing the cylinders and then calculating the change to the coefficients



	Present method	Doublet (Dalton & Helfinstine 1971)†
$[A_{ii}]^\dagger$ or $[\bar{B}_{ii}]$	$\begin{bmatrix} -1.0320 & \pm 0.2269 \\ \pm 0.2269 & -1.0320 \end{bmatrix}$	$\begin{bmatrix} -1.0313 & \pm 0.2245 \\ \pm 0.2245 & -1.0313 \end{bmatrix}$
$[D_{ii}^{(1)}] + [D_{ii}^{(2)}]$	$\begin{bmatrix} 0.3791 & -0.6550 \\ 0.6550 & -0.3791 \end{bmatrix}$	$\begin{bmatrix} 0.3534 & -0.6239 \\ 0.6239 & -0.3534 \end{bmatrix}$
$[\bar{C}_{ii}^{(1)}] + [\bar{C}_{ii}^{(2)}]$	$\begin{bmatrix} 0.1992 & -0.4751 \\ 0.4751 & -0.1992 \end{bmatrix}$	$\begin{bmatrix} 0.1915 & -0.5172 \\ 0.5172 & -0.1915 \end{bmatrix}$

† Off-diagonals are positive for A_{ii} , negative for \bar{B}_{ii} . \bar{A}_{ii} and B_{ii} both vanish in this case.
 ‡ Obtained by Mavriplis (1982), using Dalton & Helfinstine's analysis.

TABLE 4. Comparison of the inertia terms and the damping terms due solely to the unsteady part ($\partial\Phi/\partial t$) of Bernoulli's equation obtained in the present analysis with those obtained by the method of Dalton & Helfinstine (1971)

time step. It is noted that, for the particular geometry considered in this test, the C_{ii} and \bar{D}_{ii} submatrices vanish and only the off-diagonal terms of the D_{ii} and \bar{C}_{ii} submatrices need be considered. As may be seen in table 4, both the virtual- (added-) mass coefficients and the damping terms due to the time derivative of the potential function are found to be in good agreement with those obtained by the present analysis. This simple test provides substantial evidence in favour of the validity of the present solution over that of Balsa (1977).

Finally, the stiffness coefficients ((23) with $\chi = 0$) were also calculated by directly noting the changes in steady lift and drag coefficients on each cylinder as various cylinders in the array were displaced. This is the method employed by Chen (1978). His results, as well as those obtained in this work by displacing the cylinders, compare favourably with the stiffness coefficients calculated by the expressions developed in the present paper, as may be seen in the lower half of table 2.

Having tested all parts of the analysis, it may now be stated that, to the authors' knowledge, it is the first complete and correct potential-flow solution which is suitable for the analysis of closely packed array geometries, involving large numbers of cylinders.†

† Although Dalton & Helfinstine's (1971) solution is believed to agree with this work, in its present form it is limited to calculating inertial and steady lift and drag coefficients, and it is difficult to extend beyond that.

6. Calculations and results

Computations were largely confined to seven-cylinder arrays of the type shown inset in figures 3 and 4 – mainly for economy, as computational costs increase sharply with the number of cylinders in the array. Nevertheless, these arrays were considered to be sufficiently large and their geometry sufficiently general to exhibit all salient features of larger systems.† As virtually all the experimental data to which the theoretical results will be compared are for arrays with $1.3 < s_p/D < 1.5$, computations were made with the two extremum values.

In the calculations, the experimentally reasonable value of $\delta = 0.01$ was used, and $m/\rho D^2$ was varied from $O(1)$ to $O(10^5)$, the lower value corresponding to light cylinders in dense (liquid) flows and the upper one to heavy cylinders in gaseous flows.

The only other parameter that needs to be selected is χ . It is recalled that this phase angle, which is attributed to viscous effects, has been introduced heuristically, and that at present no means is available for calculating it. Nevertheless, valuable guidance may be obtained from Theodorsen's (see Bisplinghoff, Ashley & Halfman 1955; Dowell *et al.* 1980), Simpson & Flower's (1977) and Lever & Weaver's (1982) work, albeit for physical models not identical with the one proposed here; in all cases the phase lag is found to be dependent, sometimes nearly linearly, on the reduced frequency fD/U .‡ Thus, for high values of U/fD , a low value of χ would be expected, and *vice versa*. Guided by the abovementioned work and also by the observed range of critical U/fD for fluid-elastic instabilities, extensive calculations were conducted with $\chi = 0^\circ, 10^\circ$ and 30° , as shown in figures 3 and 4; the effect of χ is more extensively discussed later, in conjunction with figure 5.

The calculated theoretical dimensionless critical flow velocities U_{pc}/fD for the onset of fluid-elastic instability are shown in figures 3 and 4, where they are compared with the experimental data available from various sources. It is noted that the interstitial, so-called 'pitch', flow velocity U_p is used to define its critical counterpart U_{pc} , rather than the free-stream one U , where $U_p = U[s_p/(s_p - D)]$.|| Here it should be noted that, although it was considered desirable to segregate the data for 'normal' and 'parallel' triangular arrays (in figure 3 and 4 respectively) because of the inherently different wake structures involved (figure 1), the theoretical values are only slightly different in the two cases, as this theoretical model does not recognize these wake-related differences.

One important feature of the theoretical results is that, although those presented in figures 3 and 4 are strictly for $\delta = 0.01$, they are nonetheless representative of the results for other values of δ . For example, in the case of $s_p/D = 1.5$, $m\delta/\rho D^2 = 10$ and $\chi = 30^\circ$, U_{pc}/fD is 38.2 and 36.2 for $\delta = 0.01$ and 1 respectively; these differences are smaller for larger $m\delta/\rho D^2$ and *vice versa*. Hence, although $m/\rho D^2$ and δ are independent parameters, U_{pc}/fD is much more dependent on their product $m\delta/\rho D^2$

† Indeed, calculations of the critical flow velocity for twelve-cylinder arrays differed by only -3 to -4% from those of seven-cylinder arrays.

‡ If Simpson & Flower's interpretation of the phase lag due to viscous effects were adopted (Simpson & Flower 1977; Simpson 1983, private communication), then χ (in radians) is proportional to $\mu(2\pi fD/U_p)$, where $\mu = O(1)$. Hence, for low values of $m\delta/\rho D^2$, χ is of the order of $70^\circ-30^\circ$, and for higher $m\delta/\rho D^2$ it is of the order of $30^\circ-10^\circ$. (Reasons for not conducting calculations with $\chi > 30^\circ$ will become obvious once figure 5 has been discussed.)

|| This is done partly because U_p is physically more meaningful (at least for normal triangular arrays) and is the velocity conventionally quoted in the literature, and partly because it has been found to collapse the experimental data partially for different s_p/D .

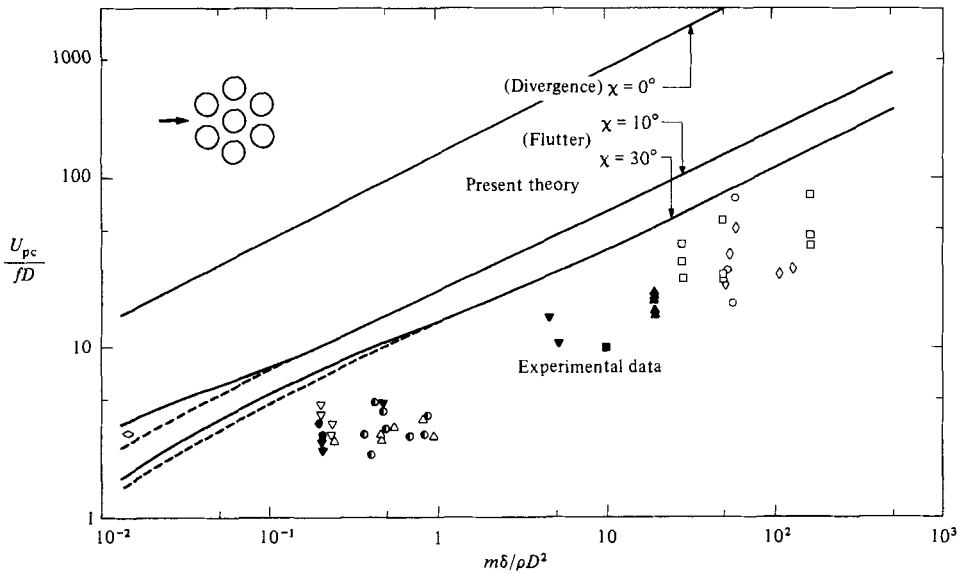


FIGURE 3. Theoretical critical flow velocities for fluid-elastic instability, calculated for the seven-cylinder normal triangular array shown and for $\delta = 0.01$: —, $s_p/D = 1.5$; ---, $s_p/D = 1.3$. Experimental data: \triangle , Chen & Jendrzejczyk (1981); \blacksquare , Connors (1980); \circ , Gibert, Chabrerie & Schlegel (1976); ∇ , Gorman (1976); \blacktriangle , Gross (1975); \square , Hartlen (1974); \bullet , Heilker & Vincent (1981); \blacktriangledown , Pettigrew *et al.* (1978); \diamond , Soper (1980); \blacklozenge , Yeung & Weaver (1983); \bullet , Žukauskas & Katinas (1980); see also Chen (1982), Paidoussis (1983).

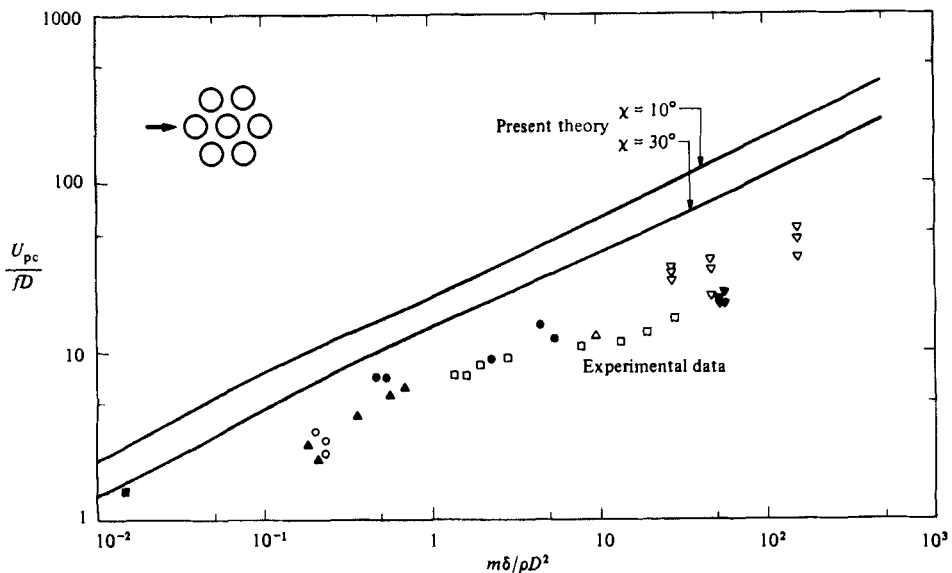


FIGURE 4. Theoretical critical flow velocities for fluid-elastic instability, calculated for the seven-cylinder, parallel (rotated) triangular array shown and for $s_p/D = 1.3$, $\delta = 0.01$. Experimental data: \triangle , Connors (1980); \circ , Gorman (1976); ∇ , Hartlen (1974); \blacktriangle , Heilker & Vincent (1981); \bullet , Pettigrew *et al.* (1978); \blacktriangledown , Soper (1980); \square , Weaver & Grover (1978); \blacksquare , Yeung & Weaver (1983); see also Chen (1982), Paidoussis (1983).

than on either separately. This agrees with Chen's (1983*b*) findings and is contrary to Weaver & El Kashlan's (1981).

It is noted that in figures 3 and 4 there are no multiple stability–instability bands at low values of $m\delta/\rho D^2$, as is the case in Lever & Weaver's (1982) and Chen's (1983*b*) work, and hence there are no 'jumps' in the overall stability diagrams. The reason for this is that in each calculation χ was taken to be a constant (albeit recognizing that it is functionally dependent on U/fD); had χ explicitly been taken as a function of U/fD – which would have required an iterative solution technique for the determination of the critical U/fD – then the trigonometric functions in (23) would have become multivalued, and hence multiple solutions for the stability boundary (at low $m\delta/\rho D^2$) would have emerged.

Another important feature of the results is that the use of U_p in preference to U has achieved the effective collapse of the theoretical results (in the two cases of s_p/D of 1.3 and 1.5), except for low values of $m\delta/\rho D^2$, as shown in figure 3.

The theoretical U_{pc}/fD for $\chi = 10^\circ$ and 30° correspond to oscillatory instabilities, and are thus directly comparable with the experimental data, whilst those for $\chi = 0^\circ$ are associated with divergence, which is a non-oscillatory instability. Hence, it is quite clear that viscous effects and the lag they introduce between cylinder displacement and the fluid forces thereby generated are quite important in the development of fluid-elastic instability.

For $\chi = 10^\circ$ and 30° the frequency at U_{pc} of the mode becoming unstable is close to its value at $U_p = 0$, which agrees with experimental observations (Païdoussis 1980, 1981); e.g., for $\chi = 30^\circ$, $m/\rho D^2 = 10^3$, $\delta = 0.01$ (so that $m\delta/\rho D^2 = 10$), $s_p/D = 1.5$, the ratio of the former to the latter frequency is 0.996. It should nevertheless be noted that this does not hold for small $m/\rho D^2$; thus, for $m/\rho D^2 = 10$, $\delta = 1$ (so that $m\delta/\rho D^2$ is still 10) and otherwise the same parameters as above, this frequency ratio is 0.597.

Comparing the theoretical results with the experimental data, it is noted that theory overestimates the critical flow velocity for instability roughly by a factor of three, for $\chi = 30^\circ$, and nearly five, for $\chi = 10^\circ$ – in an average sense, as the experimental data display a very large spread in themselves.† Here it should be noted that it would be reasonable to compare the experimental data at large $m\delta/\rho D^2$ with smaller χ than those for small $m\delta/\rho D^2$, as the former are associated with higher values of U_{pc}/fD ; this would make agreement for large $m\delta/\rho D^2$ (gaseous flows) rather worse than for small ones (liquid flows).

One of the reasons why this theory overestimates U_{pc}/fD , especially at high $m\delta/\rho D^2$, is that it does not take into account the presence of wakes and wake-interference effects on the aerodynamic-stiffness coefficients, which normally render the aerodynamic-stiffness matrix asymmetric. As shown elsewhere (Price & Païdoussis 1983), asymmetry of this matrix, which effectively means that the static force field is non-conservative, has a strong destabilizing effect on the system. This effect is entirely absent in this analysis, where this matrix is symmetric.

It is of interest that the trend in the theoretical U_{pc}/fD with increasing $m\delta/\rho D^2$ is similar to that shown by the experimental data, especially if U_{pc}/fD for $\chi = 30^\circ$ is associated with small $m\delta/\rho D^2$, and that for $\chi = 10^\circ$ or less for large $m\delta/\rho D^2$ – for

† It is noted that the experimental U_{pc}/fD and $m\delta/\rho D^2$ in many cases are calculated with values of f , m and δ *in fluid*, rather than *in vacuo* as was done in the theory. Moreover, it was found not usually possible, through insufficient information, to convert such experimental data to their *in vacuo* counterparts; this conversion would have resulted in moving the data points concerned to the left and a little lower in the case of low $m\delta/\rho D^2$ (liquid flow), but would hardly affect those with high $m\delta/\rho D^2$.

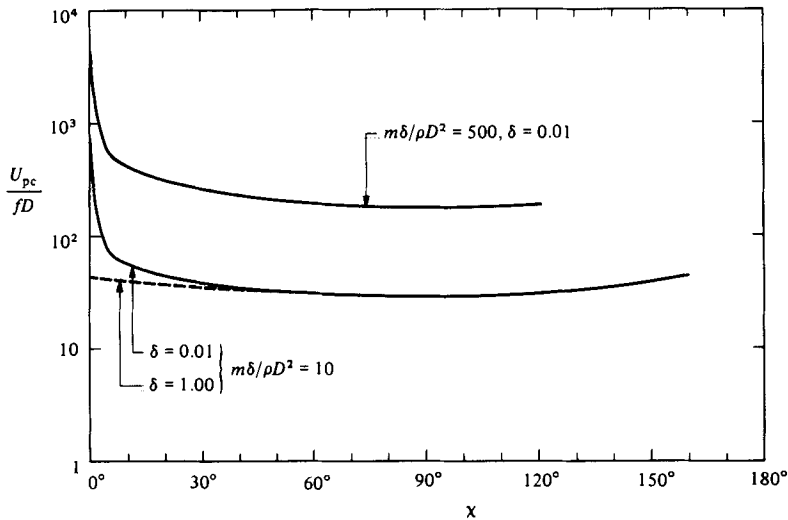


FIGURE 5. The theoretical effect of changing the phase-lag angle χ on the critical flow velocity for fluid-elastic instability, for normal triangular arrays ($s_p/D = 1.5$).

the reasons mentioned earlier. The theoretical results indicate that $U_{pc}/fD \propto (m\delta/\rho D^2)^n$, where n is in the range 0.4–0.6 almost throughout, whereas it is currently suggested that for small $m\delta/\rho D^2$ this exponent should be considerably smaller than 0.5 (Chen & Jendrzejczyk 1978).

Of course, the question arises as to how sensitive are the theoretical results presented thus far to the value of the parameter χ . As shown in figure 5, they are not so sensitive – at least in the range $5^\circ < \chi < 160^\circ$. For $\chi < 5^\circ$ approximately, however, the critical flow velocity for lightly damped systems increases sharply as $\chi = 0^\circ$ is approached. (At $\chi = 0^\circ$, as previously mentioned, the very nature of the instability is different.) This effect is nevertheless attenuated by higher damping, as shown. For $\chi = 180^\circ$, no instability is found at all; the situation here is similar to that for $\chi = 0^\circ$, except that the signs of all flow-induced stiffness terms are reversed. It is recalled at this point that, in the calculation of the terms associated with phase lag (23), the frequency of oscillation at the threshold of instability was taken as the natural frequency of the cylinders. For very low values of χ or $m/\rho D^2$ this may indeed alter the shape of figure 5. However, the results for $\chi = 0^\circ$ (divergence) are unaffected, since these terms then vanish in any case.

Considering the drastic simplifying assumptions that have been made in the theory, the most serious of which is to ignore the wakes – the existence of viscous effects being recognized only through the introduction of the phase lag χ – it is remarkable that the theoretical values of U_{pc}/fD for $\chi = 30^\circ$ or 10° are as close to the experimental values as they are. Of course, prediction of the critical flow velocity to within a factor of 3 or 5 is not satisfactory. Nevertheless, this lack of success should be viewed in the context of existing semi-empirical analytical models, relying heavily on measured force coefficient data, which are capable of prediction to just within a factor of 2.†

One current controversy is concerned with whether one flexible cylinder surrounded

† In considering the success, or lack thereof, of this theoretical model in terms of predicting U_{pc}/fD much more emphasis should be placed on figure 3 than on figure 4, for the reasons stated at the outset. The fact that agreement between theory and experiment is similar in the two cases could well be fortuitous.

by rigid ones does become unstable for high $m\delta/\rho D^2$ – it being generally accepted that it does for low $m\delta/\rho D^2$ (Lever & Weaver 1982; Chen 1983*b*; Paidoussis 1983). Calculations conducted for one flexible cylinder surrounded by six rigid ones showed that, according to this theory, the flexible cylinder does become unstable for all $m\delta/\rho D^2$ – but at higher critical flow velocities (by 30–75%), as compared with the system with seven flexible cylinders.

7. Conclusion

A potential-flow theory has been presented for the dynamics, and more specifically the fluid-elastic instabilities, of staggered arrays of cylinders in cross-flow. The theory is purely analytical, except for the empirical parameter χ , which is a measure of the phase lag between displacement of the cylinders and the lift and drag forces generated on them – owing to viscous effects, otherwise neglected.

All analytical parts of the theory were carefully checked and compared with previous work. Contradictions between previous solutions have been exposed, and to some degree resolved, in the present work; hence, to the authors' knowledge, this represents the first successful formulation of the problem in terms of potential-flow theory. In one sense, this is considered to be the major accomplishment of this work, as it permitted the assessment of the limitations of potential-flow theory for predicting the dynamical behaviour of the system.

The most important finding of this work is that, if viscous effects are neglected altogether, then the only form of instability possible is divergence, which is a static, non-oscillatory instability. Hence, having established the prominence of the viscous effects, it was considered desirable to take them into account, albeit heuristically. Although no attempt was made to determine the viscous forces *per se*, one important *effect* of these forces was introduced: the phase lag χ . It was found that, with reasonable values of this phase lag, theory predicts the occurrence of oscillatory instabilities; moreover, the predicted characteristics of the system and the threshold of instability are remarkably close to the measured ones – remarkably, that is, considering the degree of idealization entailed in the analytical model.

The above suggests that a useful direction for future research could be to attempt the analytical modelling of viscous forces on the cylinders, and hence the determination of the phase lag inherent therein.

It is nevertheless recognized that ideal-flow theory is not the most suitable fluid-mechanical tool for a successful theory for the problem at hand, because of the importance of the wakes – even on the quasi-static fluid-dynamic-stiffness coefficients. Thus, unless wake-interference effects are accounted for, the essential non-conservativeness of the force field (in the static sense), which is known to have a strong destabilizing influence on the dynamics of the system, is not recognized.

Finally, it might be useful to discuss this theoretical model in the context of other, recently published theories. Price & Paidoussis' (1983) theory requires the measurement of the static forces on the cylinders in various displaced positions, and Tanaka & Takahara (1981) and Chen's (1983*b*) theory requires the measurement of the *dynamic* forces over a range of flow velocities – a difficult and tedious task. Lever & Weaver's (1982) theory requires three empirical inputs, and is otherwise analytical; it is therefore more comparable to this theory, which involves but one empirical parameter. As expected, the more empirical input introduced in the analytical model, the more 'successful' it is likely to be in terms of prediction of fluid-elastic instabilities.

The authors gratefully acknowledge support by the Natural Sciences and Engineering Research Council of Canada and Le Programme ‘Formation de chercheurs et action concertée’ of Québec, which has made this research possible. They also acknowledge Professor B. G. Newman for graciously making available to them the facilities of his Low Speed Aerodynamics Laboratory and some useful discussions, and Mr Phuong Luu for undertaking some of the computations, the results of which are presented in this paper.

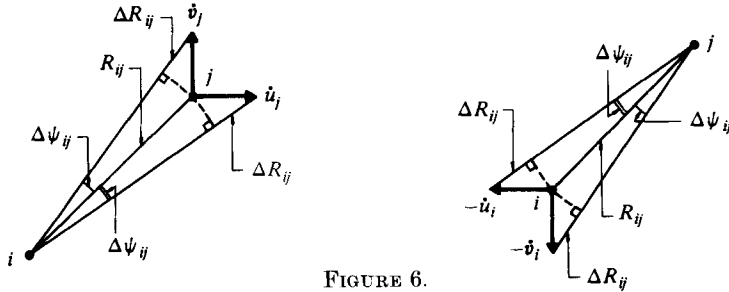


FIGURE 6.

Appendix A. Evaluation of some terms in equation (14) for $\partial\Phi/\partial t$

Equation (16) gives the expression for α_{jnl} ; similar expressions may be written for γ_{jnl} , β_{jnl} and δ_{jnl} . The procedure for evaluation of these quantities will only be illustrated through the first.

The first of (8) may be differentiated with respect to time and the resulting differential evaluated at the cylinder equilibrium positions (i.e. $r'_i = r_i$, $\theta'_i = \theta_i$, $R'_{ij} = R_{ij}$, $\psi'_{ij} = \psi_{ij}$), yielding

$$\begin{aligned}
 &(-n)\dot{\alpha}_{inl} + \sum_{j=1}^K \sum_{m=1}^{\infty} G_{mni} \{ \dot{\alpha}_{jml} \cos(m+n)\psi_{ij} + \delta_{jml} \sin(m+n)\psi_{ij} \} \\
 &= \sum_{j=1}^K \sum_{m=1}^{\infty} \frac{(-1)^m (m+n)!}{(m-1)!(n-1)!} \frac{R^{m+n}}{R_{ij}^{m+n+1}} \{ [\alpha_{jml} \cos(m+n)\psi_{ij} + \delta_{jml} \sin(m+n)\psi_{ij}] \dot{R}_{ij} \\
 &\quad + [\alpha_{jml} \sin(m+n)\psi_{ij} - \delta_{jml} \cos(m+n)\psi_{ij}] \dot{\psi}_{ij} R_{ij} \}. \tag{A 1}
 \end{aligned}$$

From figure 6 it may be seen that

$$\dot{R}_{ij} = (\dot{u}_j - \dot{u}_i) \cos \psi_{ij} + (\dot{v}_j - \dot{v}_i) \sin \psi_{ij} \tag{A 2}$$

and $R_{ij} \dot{\psi}_{ij} = -(\dot{u}_j - \dot{u}_i) \sin \psi_{ij} + (\dot{v}_j - \dot{v}_i) \cos \psi_{ij}.$ (A 3)

Substituting into (A 1) yields

$$\begin{aligned}
 &(-n)\dot{\alpha}_{inl} + \sum_{j=1}^K \sum_{m=1}^{\infty} G_{mni} \{ \dot{\alpha}_{jml} \cos(m+n)\psi_{ij} + \delta_{jml} \sin(m+n)\psi_{ij} \} \\
 &= \sum_{j=1}^K \sum_{m=1}^{\infty} \frac{(-1)^{m'} (m'+n)!}{(m'-1)!(n-1)!} \frac{R^{m'+n}}{R_{ij}^{m'+n+1}} \\
 &\quad \times \{ \alpha_{j'm'l} \cos(m'+n+1)\psi_{ij'} + \delta_{j'm'l} \sin(m'+n+1)\psi_{ij'} \} \left(\frac{\partial u_{j'}}{\partial t} - \frac{\partial u_i}{\partial t} \right) \\
 &\quad + \sum_{j=1}^K \sum_{m=1}^{\infty} \frac{(-1)^{m'} (m'+n)!}{(m'-1)!(n-1)!} \frac{R^{m'+n}}{R_{ij}^{m'+n+1}} \\
 &\quad \times \{ \alpha_{j'm'l} \sin(m'+n+1)\psi_{ij'} - \delta_{j'm'l} \cos(m'+n+1)\psi_{ij'} \} \left(\frac{\partial v_{j'}}{\partial t} - \frac{\partial v_i}{\partial t} \right). \tag{A 4}
 \end{aligned}$$

Hence, substituting (16) and the equivalent expression for δ_{jnl} into (A 4), one obtains an equation of the form

$$\begin{aligned} & \sum_{l'=1}^K \left\{ (-n) \frac{\partial \alpha_{inl}}{\partial u_{l'}} + \sum_{j=1}^K \sum_{m=1}^{\infty} G_{mnij} \left\{ \frac{\partial \alpha_{jnl}}{\partial u_{l'}} \cos(m+n) \psi_{ij} + \frac{\partial \delta_{jnl}}{\partial u_{l'}} \sin(m+n) \psi_{ij} \right\} \frac{\partial u_{l'}}{\partial t} \right\} \\ & + \sum_{l'=1}^K \left\{ \text{terms involving } \frac{\partial v_{l'}}{\partial t} \right\} \\ & = \sum_{j=1}^K \sum_{m'=1}^{\infty} \frac{(-1)^{m'} (m'+n)! R^{m'+n}}{(m'-1)! (n-1)! R_{ij}^{m'+n+1}} \\ & \quad \times \left\{ \alpha_{j'm'l} \cos(m'+n+1) \psi_{ij'} + \delta_{j'm'l} \sin(m'+n+1) \psi_{ij'} \right\} \left(\frac{\partial u_{j'}}{\partial t} - \frac{\partial u_i}{\partial t} \right) \\ & + \left\{ \text{terms involving } \left(\frac{\partial v_{j'}}{\partial t} - \frac{\partial v_i}{\partial t} \right) \right\}. \end{aligned} \tag{A 5}$$

Since the above must hold for all possible values of the set $\dot{u}_{l'}, \dot{v}_{l'}$, the latter are linearly independent, and thus (A 5) may be reduced to equating the coefficients of $\dot{u}_{l'}, \dot{v}_{l'}$ on either side of the equation; thus

$$\begin{aligned} & (-n) \frac{\partial \alpha_{inl}}{\partial u_{l'}} + \sum_{j=1}^K \sum_{m=1}^{\infty} G_{mnij} \left\{ \frac{\partial \alpha_{jnl}}{\partial u_{l'}} \cos(m+n) \psi_{ij} + \frac{\partial \delta_{jnl}}{\partial u_{l'}} \sin(m+n) \psi_{ij} \right\} \\ & = \sum_{m'=1}^{\infty} \frac{(-1)^{m'} (m'+n)! R^{m'+n}}{(m'-1)! (n-1)! R_{il'}^{m'+n+1}} \{ \alpha_{l'm'l} \cos(m'+n+1) \psi_{il'} + \delta_{l'm'l} \\ & \quad \times \sin(m'+n+1) \psi_{il'} \}, \end{aligned} \tag{A 6}$$

and a similar expression holds for $\partial \alpha_{inl} / \partial v_{l'}$. A different procedure must be utilized for $l' = i$, but will not be presented here for brevity. Similar expressions for the derivatives of δ_{inl} may also be written, leading to the set

$$(-n) \left(\frac{\partial \alpha_{inl}}{\partial u_{l'}} \right) + \sum_{j=1}^K \sum_{m=1}^{\infty} G_{mnij} \left\{ \frac{\partial \alpha_{jnl}}{\partial u_{l'}} \cos(m+n) \psi_{ij} + \frac{\partial \delta_{jnl}}{\partial u_{l'}} \sin(m+n) \psi_{ij} \right\} = P_{inl'}. \tag{A 7a}$$

$$(-n) \left(\frac{\partial \delta_{inl}}{\partial u_{l'}} \right) + \sum_{j=1}^K \sum_{m=1}^{\infty} G_{mnij} \left\{ \frac{\partial \alpha_{jnl}}{\partial u_{l'}} \sin(m+n) \psi_{ij} - \frac{\partial \delta_{jnl}}{\partial u_{l'}} \cos(m+n) \psi_{ij} \right\} = Q_{inl'} \tag{A 7b}$$

$$(-n) \left(\frac{\partial \alpha_{inl}}{\partial v_{l'}} \right) + [\text{similar terms as in (A 7a)}] = \bar{P}_{inl'}, \tag{A 8a}$$

$$(-n) \left(\frac{\partial \delta_{inl}}{\partial v_{l'}} \right) + [\text{similar terms as in (A 7b)}] = \bar{Q}_{inl'}, \tag{A 8b}$$

where

$$\left. \begin{aligned} P_{inl'} &= \sum_{m'=1}^{\infty} \frac{(-1)^{m'} (m'+n)! R^{m'+n}}{(m'-1)! (n-1)! R_{il'}^{m'+n+1}} [\alpha_{l'm'l} \cos(m'+n+1) \psi_{il'} + \delta_{l'm'l} \sin(m'+n+1) \psi_{il'}], \\ Q_{inl'} &= \sum_{m'=1}^{\infty} \frac{(-1)^{m'} (m'+n)! R^{m'+n}}{(m'-1)! (n-1)! R_{il'}^{m'+n+1}} [\alpha_{l'm'l} \sin(m'+n+1) \psi_{il'} - \delta_{l'm'l} \cos(m'+n+1) \psi_{il'}], \\ \bar{P}_{inl'} &= Q_{inl'}, \quad \bar{Q}_{inl'} = P_{inl'}. \end{aligned} \right\} \tag{A 9}$$

for $l \neq i$, whilst for $l = i$ the following must be employed:

$$P_{inli} = -\sum_{j=1}^K P_{inlj}, \quad Q_{inli} = -\sum_{j=1}^K Q_{inlj}. \quad (A 10)$$

The set of equations (A 7) and (A 8), separately, may be written in matrix form and then solved, yielding $\partial\alpha_{jnl}/\partial u_{l'}$, $\partial\delta_{jnl}/\partial u_{l'}$, etc.; with these known, then α_{jnl} , δ_{jnl} , etc. are known, and therefore \dot{a}_{jn} and \dot{b}_{jn} of (15).

Appendix B. Some constants obtained in the analysis

The constants involved in (19) are given by

$$A_{il} = 2\alpha_{i1l} + \delta_{il}, \quad B_{il} = 2\gamma_{i1l}, \quad \bar{A}_{il} = 2\delta_{i1l}, \quad \bar{B}_{il} = 2\beta_{i1l} + \delta_{il}, \quad (B 1)$$

where δ_{il} is Kronecker's delta;

$$\begin{aligned} C_{il}^{(1)} = & -\pi \sum_{l=1}^K \left[\frac{\partial\alpha_{i1l}}{\partial u_{l'}} \cos \psi_0 + \frac{\partial\gamma_{i1l}}{\partial u_{l'}} \sin \psi_0 \right] \\ & + \sum_{j=1}^K \sum_{n=1}^{\infty} (-1)^n n \left(\frac{R}{R_{ij}} \right)^{n+1} \left\{ \left[\frac{\partial\alpha_{jnl}}{\partial u_{l'}} \cos \psi_0 + \frac{\partial\gamma_{jnl}}{\partial u_{l'}} \sin \psi_0 \right] \cos(n+1)\psi_{ij} \right. \\ & \left. + \left[\frac{\partial\delta_{jnl}}{\partial u_{l'}} \cos \psi_0 + \frac{\partial\beta_{jnl}}{\partial u_{l'}} \sin \psi_0 \right] \sin(n+1)\psi_{ij} \right\}, \quad (B 2a) \end{aligned}$$

$$\begin{aligned} \bar{C}_{il}^{(1)} = & -\pi \sum_{l=1}^K \left[\frac{\partial\delta_{i1l}}{\partial u_{l'}} \cos \psi_0 + \frac{\partial\beta_{i1l}}{\partial u_{l'}} \sin \psi_0 \right] \\ & + \sum_{j=1}^K \sum_{n=1}^{\infty} (-1)^n n \left(\frac{R}{R_{ij}} \right)^{n+1} \left\{ \left[\frac{\partial\alpha_{jnl}}{\partial u_{l'}} \cos \psi_0 + \frac{\partial\gamma_{jnl}}{\partial u_{l'}} \sin \psi_0 \right] \sin(n+1)\psi_{ij} \right. \\ & \left. - \left[\frac{\partial\delta_{jnl}}{\partial u_{l'}} \cos \psi_0 + \frac{\partial\beta_{jnl}}{\partial u_{l'}} \sin \psi_0 \right] \cos(n+1)\psi_{ij} \right\}; \quad (B 2b) \end{aligned}$$

the $D_{il}^{(1)}$ and $\bar{D}_{il}^{(1)}$ terms may be obtained by replacing $\partial/\partial u_{l'}$ by $\partial/\partial v_{l'}$ in the above expressions;

$$C_{il}^{(2)} = \sum_{n=1}^{\infty} \left\{ (-1)^n n(n+1) \pi \left(\frac{R}{R_{il}} \right)^{n+2} [\Gamma_{ln} \cos(n+2)\psi_{il} + A_{ln} \sin(n+2)\psi_{il}] \right\} (1 - \delta_{il}), \quad (B 3a)$$

$$D_{il}^{(2)} = \sum_{n=1}^{\infty} \left\{ (-1)^n n(n+1) \pi \left(\frac{R}{R_{il}} \right)^{n+2} [\Gamma_{ln} \sin(n+2)\psi_{il} - A_{ln} \cos(n+2)\psi_{il}] \right\} (1 - \delta_{il}), \quad (B 3b)$$

$$\bar{C}_{il}^{(2)} = D_{il}^{(2)}, \quad \bar{D}_{il}^{(2)} = -C_{il}^{(2)}, \quad (B 3c)$$

where

$$\Gamma_{ln} = \sum_{j=1}^K [\alpha_{lnj} \cos \psi_0 + \gamma_{lnj} \sin \psi_0], \quad A_{ln} = \sum_{j=1}^K [\delta_{lnj} \cos \psi_0 + \beta_{lnj} \sin \psi_0]. \quad (B 4)$$

It is of interest that, for $i = l$, $C_{il}^{(2)} = D_{il}^{(2)} = 0$; hence there is no velocity-dependent force due to motion of the cylinder itself, but only due to motion of neighbouring cylinders. Although the surface-pressure distribution on the cylinder is altered by its own motion, when integrated around the circumference it gives no net effect; this is in agreement with single-cylinder results.

The constants involved in (20) are given by Mavriplis (1982):

$$C_{\text{Doi}} = \frac{1}{4}\pi \sum_{n=1}^{\infty} \sum_{l=1}^K \left\{ 2\delta_{n2} \{ C_{inl}^* \cos^2 \psi_0 - B_{inl}^* \sin^2 \psi_0 - (A_{inl}^* - D_{inl}^*) \cos \psi_0 \sin \psi_0 \} \right. \\ \left. + \sum_{l'=1}^K \{ D1_{inll'} \cos^2 \psi_0 + D2_{inll'} \sin^2 \psi_0 + (D3_{inll'} + D4_{inll'}) \cos \psi_0 \sin \psi_0 \} \right\}, \quad (\text{B } 5a)$$

$$C_{\text{Loi}} = \frac{1}{4}\pi \sum_{n=1}^{\infty} \sum_{l=1}^K \left\{ -2\delta_{n2} \{ A_{inl}^* \cos^2 \psi_0 + D_{inl}^* \sin^2 \psi_0 + (C_{inl}^* + B_{inl}^*) \cos \psi_0 \sin \psi_0 \} \right. \\ \left. + \sum_{l'=1}^K \{ D5_{inll'} \cos^2 \psi_0 + D6_{inll'} \sin^2 \psi_0 + (D7_{inll'} + D8_{inll'}) \cos \psi_0 \sin \psi_0 \} \right\}, \quad (\text{B } 5b)$$

$$C_{il}^{(3)} = \frac{1}{4}\pi \sum_{n=1}^{\infty} \left\{ 2\delta_{n2} (A_{inl}^* \sin \psi_0 - C_{inl}^* \cos \psi_0) \right. \\ \left. - \sum_{l'=1}^K \{ (D1_{inll'} + D1_{inl'l}) \cos \psi_0 + (D3_{inll'} + D4_{inll'}) \sin \psi_0 \} \right\}, \quad (\text{B } 5c)$$

$$D_{il}^{(3)} = \frac{1}{4}\pi \sum_{n=1}^{\infty} \left\{ 2\delta_{n2} (B_{inl}^* \sin \psi_0 - D_{inl}^* \cos \psi_0) \right. \\ \left. - \sum_{l'=1}^K \{ (D3_{inll'} + D4_{inl'l}) \cos \psi_0 + (D2_{inll'} + D2_{inl'l}) \sin \psi_0 \} \right\}, \quad (\text{B } 5d)$$

$$\bar{C}_{il}^{(3)} = \frac{1}{4}\pi \sum_{n=1}^{\infty} \left\{ 2\delta_{n2} (A_{inl}^* \cos \psi_0 + C_{inl}^* \sin \psi_0) \right. \\ \left. - \sum_{l'=1}^K \{ (D5_{inll'} + D5_{inl'l}) \cos \psi_0 + (D7_{inll'} + D8_{inll'}) \sin \psi_0 \} \right\}, \quad (\text{B } 5e)$$

$$\bar{D}_{il}^{(3)} = \frac{1}{4}\pi \sum_{n=1}^{\infty} \left\{ 2\delta_{n2} (B_{inl}^* \cos \psi_0 + D_{inl}^* \sin \psi_0) \right. \\ \left. - \sum_{l'=1}^K \{ (D7_{inll'} + D8_{inl'l}) \cos \psi_0 + (D6_{inll'} + D6_{inl'l}) \sin \psi_0 \} \right\}, \quad (\text{B } 5f)$$

where

$$\left. \begin{aligned} D1_{inll'} &= A_{inl}^* (A_{in+1l'}^* + A_{in-1l'}^*) + C_{inl}^* (C_{in+1l'}^* + C_{in-1l'}^*), \\ D2_{inll'} &= B_{inl}^* (B_{in+1l'}^* + B_{in-1l'}^*) + D_{inl}^* (D_{in+1l'}^* + D_{in-1l'}^*), \\ D3_{inll'} &= B_{inl}^* (A_{in+1l'}^* + A_{in-1l'}^*) + D_{inl}^* (C_{in+1l'}^* + C_{in-1l'}^*), \\ D4_{inll'} &= A_{inl}^* (B_{in+1l'}^* + B_{in-1l'}^*) + C_{inl}^* (D_{in+1l'}^* + D_{in-1l'}^*), \\ D5_{inll'} &= A_{inl}^* (C_{in+1l'}^* - C_{in-1l'}^*) - C_{inl}^* (A_{in+1l'}^* - A_{in-1l'}^*), \\ D6_{inll'} &= B_{inl}^* (D_{in+1l'}^* - D_{in-1l'}^*) - D_{inl}^* (B_{in+1l'}^* - B_{in-1l'}^*), \\ D7_{inll'} &= B_{inl}^* (C_{in+1l'}^* - C_{in-1l'}^*) - D_{inl}^* (A_{in+1l'}^* - A_{in-1l'}^*), \\ D8_{inll'} &= A_{inl}^* (D_{in+1l'}^* - D_{in-1l'}^*) - C_{inl}^* (B_{in+1l'}^* - B_{in-1l'}^*), \end{aligned} \right\} \quad (\text{B } 6)$$

and A_{inl}^* , B_{inl}^* , C_{inl}^* , D_{inl}^* are related to the α_{inl} , β_{inl} , γ_{inl} , δ_{inl} of (8) by

$$\left. \begin{aligned} A_{inl}^* &= 2n\delta_{inl}, & B_{inl}^* &= 2n\beta_{inl} + \delta_{n1}\delta_{il}, \\ C_{inl}^* &= -2n\alpha_{inl} - \delta_{n1}\delta_{il}, & D_{inl}^* &= -2n\gamma_{inl}; \end{aligned} \right\} \quad (\text{B } 7)$$

as before, the doubly subscripted δ s are Kronecker deltas.

Finally, the partial-derivative terms in (21) are given by the corresponding derivatives of the terms in (B 5). Thus

$$\frac{\partial C_{Doi}}{\partial u_p} = \frac{\pi}{4} \sum_{n=1}^{\infty} \sum_{l=1}^K \left\{ 2\delta_{n2} \left[\frac{\partial C_{inl}^*}{\partial u_p} \cos^2 \psi_0 - \frac{\partial B_{inl}^*}{\partial u_p} \sin^2 \psi_0 + \text{etc.} \right] + \sum_{l'=1}^K \left[\frac{\partial D1_{inll'}}{\partial u_p} \cos^2 \psi_0 + \frac{\partial D2_{inll'}}{\partial u_p} \sin^2 \psi_0 + \dots \text{etc.} \right] \right\}, \quad (\text{B } 8)$$

where partial derivatives of (B 6) are also involved, and

$$\frac{\partial A_{inl}^*}{\partial u_p} = 2n \frac{\partial \delta_{inl}}{\partial u_p}, \quad \frac{\partial B_{inl}^*}{\partial u_p} = 2n \frac{\partial \beta_{inl}}{\partial u_p}, \quad \frac{\partial C_{inl}^*}{\partial u_p} = -2n \frac{\partial \alpha_{inl}}{\partial u_p}, \quad \frac{\partial D_{inl}^*}{\partial u_p} = -2n \frac{\partial \gamma_{inl}}{\partial u_p}, \quad (\text{B } 9)$$

with similar expressions for the v_l derivatives. It is recalled that $\partial \alpha_{inl} / \partial u_p$ and similar terms have already been determined through (A 7)–(A 10).

REFERENCES

- BALSA, T. F. 1977 *J. Sound Vib.* **50**, 285.
- BISHOP, R. E. & JOHNSON, D. C. 1960 *The Mechanics of Vibration*. Cambridge University Press.
- BISPLINGHOFF, R. L., ASHLEY, H. & HALFMAN, R. L. 1955 *Aeroelasticity*. Addison-Wesley.
- BLEVINS, R. D. 1974 *Trans. ASME. J: J. Pressure Vessel Tech.* **96**, 263.
- BLEVINS, R. D. 1977 *Trans. ASME. I: J. Fluids Engng* **99**, 457.
- CHEN, S. S. 1978 *Nucl. Engng & Design* **47**, 67.
- CHEN, S. S. 1982 In *Proc. BHRA Intl Conf. on Flow Induced Vibrations in Fluid Engineering, Reading, U.K.*; Paper F2, p. 233.
- CHEN, S. S. 1983a *Trans. ASME: J. Vib., Acoust., Stress & Reliab. Design* **105**, 51. (ASME Paper 81-DET-21).
- CHEN, S. S. 1983b *Trans. ASME: J. Vib., Acoust., Stress & Reliab. Design* **105**, 253. (ASME Paper 81-DET-22).
- CHEN, S. S. & JENDRZEJCZYK, J. A. 1981 *J. Sound Vib.* **78**, 355.
- CONNORS, H. J. 1970 In *Flow-Induced Vibration in Heat Exchangers* (ed. D. D. Reiff), p. 42. ASME.
- CONNORS, H. J. 1980 In *Flow-Induced Vibration of Power Plant Components* (ed. M. K. Au-Yang), p. 93. ASME.
- DALTON, C. & HELFINSTINE, R. A. 1971 *Trans. ASME D: J. Basic Engng* **93**, 636.
- DEN HARTOG, J. P. 1932 *Trans AIEE* **51**, 1074.
- DOWELL, E. H., CURTISS, H. C., SCANLAN, R. H. & SISTO, F. 1980 *A Modern Course in Aeroelasticity*. Sijthoff & Noordhoff.
- GIBERT, R. J., CHABRERIE, J. & SCHLEGEL, R. 1976 *DGRST Etude 4870 CR No. 1*. Commissariat à l'Energie Atomique, France.
- GORMAN, D. J. 1976 *Nucl. Sci. Engng* **61**, 324.
- GROSS, H. G. 1975 Untersuchung aeroelastischer Schwingungsmechanismen und deren Berücksichtigung bei der Auslegung von Rohrbündel-Wärmetauschern. Ph.D. dissertation, Technical University Hanover.
- HARTLEN, R. T. 1974 *Ontario Hydro Rep.* 74-309-K.
- HEILKER, W. J. & VINCENT, R. Q. 1981 *Trans. ASME A: J. Engng Power* **103**, 358.
- HEINECKE, E. P. & MOHR, K. H. 1982 *Proc. UKAEA/BNES 3rd Keswick Intl Conf. Vibration in Nuclear Plant, Keswick, U.K.*; Paper 1.2, p. 25.
- LEVER, J. H. & WEAVER, D. S. 1982 In *Flow-Induced Vibration of Circular Cylindrical Structures 1982* (ed. S. S. Chen, M. P. Paidoussis & M. K. Au-Yang), p. 87. ASME.
- MAVRIPLIS, D. 1982 An investigation of the limitations of potential flow in cross-flow induced vibrations of cylindrical arrays. M.Eng. thesis, McGill University.
- PAÏDOUSSIS, M. P. 1966a *J. Fluid Mech.* **26**, 717.
- PAÏDOUSSIS, M. P. 1966b *J. Fluid Mech.* **26**, 737.
- PAÏDOUSSIS, M. P. 1979 *J. Sound Vib.* **65**, 391.

- PAÏDOUSSIS, M. P. 1980 In *Practical Experiences with Flow-Induced Vibrations* (ed. E. Naudascher & D. Rockwell), p. 1. Springer.
- PAÏDOUSSIS, M. P. 1981 *J. Sound Vib.* **76**, 329.
- PAÏDOUSSIS, M. P. 1983 *Nucl. Engng & Design* **74**, 31.
- PAÏDOUSSIS, M. P. & SUSS, S. 1977 *Trans. ASME E: J. Appl. Mech.* **44**, 401.
- PETTIGREW, M. J. & GORMAN, D. J. 1978 In *Proc. BNES Intl Conf. Vibration in Nuclear Plant, Keswick, U.K.: Paper 2.3*.
- PETTIGREW, M. J., SYLVESTRE, Y. & CAMPAGNA, A. O. 1978 *Nucl. Engng & Design* **48**, 97.
- PRICE, S. J. & PAÏDOUSSIS, M. P. 1982 In *Proc. UKAEA/BNES 3rd Keswick Intl Conf. Vibration in Nuclear Plant, Keswick, U.K.; Paper 1.7*, p. 107.
- PRICE, S. J. & PAÏDOUSSIS, M. P. 1983 *Trans. ASME J. Vib., Acoust., Stress & Reliab. Design* **105**, 59. (*ASME Paper 81-DET-24*).
- ROBERTS, B. W. 1962 Low frequency self-excited vibration in a row of circular cylinders mounted in an air stream. Ph.D. thesis, University of Cambridge.
- ROBERTS, B. W. 1966 *Mech. Engng Sci. Monograph* No. 4. I.Mech.E., London.
- SIMPSON, A. & FLOWER, J. W. 1977 *J. Sound Vib.* **51**, 183.
- SOPER, B. M. 1980 In *Flow-Induced Heat Exchanger Tube Vibration - 1980* (ed. J. M. Chenoweth & J. R. Stenner), p. 1. ASME.
- SUSS, S. 1977 Stability of a cluster of flexible cylinders in bounded axial flow. M.Eng. thesis, McGill University.
- TANAKA, H. & TAKAHARA, S. 1981 *J. Sound Vib.* **77**, 19.
- WALLIS, R. P. 1939 *Engineering* **148**, 423.
- WEAVER, D. S. & EL KASHLAN, M. 1981 *J. Sound Vib.* **76**, 283.
- WEAVER, D. S. & GROVER, L. K. 1978 *J. Sound Vib.* **59**, 277.
- WHITE, F. M. 1979 *Fluid Mechanics*. McGraw Hill.
- YEUNG, H. C. & WEAVER, D. S. 1983 *Trans. ASME: J. Vib., Acoust., Stress & Reliab. Design* **105**, 76. (*ASME Paper 81-DET-25*).
- ŽUKAUSKAS, A. & KATINAS, V. 1980 In *Practical Experiences with Flow-Induced Vibrations* (ed. E. Naudascher & D. Rockwell), p. 188. Springer.